AGE (2015) 37: 102
DOI 10.1007/s11357-015-9839-0

Chronic adjunction of 1-deoxynojirimycin protects from age-related behavioral and biochemical changes in the SAMP8 mice

Gui-Hai Chen · Jing-Jing Tong · Fang Wang · Xue-Qin Hu · Xue-Wei Li · Fei Tao · Zhao-Jun Wei

Received: 19 June 2015 / Accepted: 15 September 2015 / Published online: 23 September 2015

Abstract Several studies have indicated that a caloric restriction mimetic or treatment for type 2 diabetes may reverse brain aging. Therefore, we investigated the effect of 1-deoxynojirimycin (DNJ), an alkaloid acting as an inhibitor of α-glucosidase, on age-related behavioral and biochemical changes. SAMP8 mice were randomly assigned to a control group labeled "old" or to the 10- or 20-mg/kg/day DNJ groups. The mice in the DNJ groups were administered DNJ orally from 3 to 9 months of age, and then, a "young" control group was added to analyze the age effect. The old controls exhibited significant declines in sensorimotor ability, open-field anxiety, spatial and nonspatial memory abilities, and age-related biochemical changes, including decreased serum insulin level; increased levels of insulin-like growth factor 1 receptor, presynaptic protein synaptotagmin-1, and astrocyte activation; and decreased levels of insulin receptor, brain-derived neurotrophic factor, presynaptic protein syntaxin-1, and acetylation of histones H4 at lysine 8 in the dorsal hippocampus. Significant correlations exist between the age-related behavioral deficits and the serological and histochemical data. Chronic DNJ treatment alleviated these age-related changes, and the 20-mg/kg/day DNJ group showed more significant improvement. Thus, DNJ may have the potential to maintain successful brain aging.

Keywords BDNF · Brain aging · 1-Deoxynojirimycin · Histone acetylation · Insulin receptor · Learning and memory

Gui-Hai Chen and Jing-Jing Tong contributed equally to this work.

Electronic supplementary material The online version of this article (doi:10.1007/s11357-015-9839-0) contains supplementary material, which is available to authorized users.

G.-H. Chen (✉)
Department of Neurology, the Affiliated Chaohu Hospital of Anhui Medical University, Chaohu, Hefei 238000, People's Republic of China
e-mail: doctorcgh@163.com

G.-H. Chen · X.-Q. Hu · Z.-J. Wei (✉)
School of Biotechnology and Food Engineering, Hefei University of Technology, Hefei 230009 Anhui, People's Republic of China
e-mail: zjwei@hfut.edu.cn

J.-J. Tong
Department of Rheumatism and Immunity, the First Affiliated Hospital of Anhui Medical University, Hefei 230022, People's Republic of China

G.-H. Chen · J.-J. Tong · F. Wang · X.-W. Li · F. Tao
Department of Neurology, the First Affiliated Hospital of Anhui Medical University, Hefei 230022, People's Republic of China

Introduction

Aging is associated with the deterioration of cognitive performance and motor ability and an increased incidence of neurodegenerative disorders, such as Alzheimer's dementia (AD) and Parkinson's disease (Driscoll et al. 2003). As no effective treatment is available for these diseases, approaches that alleviate brain aging and age-related pathogenesis are urgently needed.

Studies have shown that brain aging is associated with metabolic changes, such as disturbances in the insulin level and glucose homeostasis and decreases in insulin receptor (InsR), insulin-like growth factor-1 (IGF-1), and brain-derived neurotrophic factor (BDNF) in the brain (Barzilai et al. 2012). Insulin signaling in the brain is critical for metabolic function, the survival of neurons and glia, and cognitive function (Avogaro et al. 2010). InsR is densely expressed in the brain regions involved in learning and memory, including the olfactory bulb, cerebral cortex, and hippocampus (Watson and Craft 2003), and is modulated by memory activity. Animal studies have found that after completing a spatial memory task, InsR expression increases in the dentate gyrus (DG) and the CA1 subregion of the hippocampus (Abbott et al. 1999; Zhao et al. 1999). Emerging evidence suggests that insulin plays important roles in the modulation of synaptic transmission and long-term potentiation (Zhao et al. 2004). Insulin deficiency or insulin resistance can lead to neural energy deficiencies, vulnerability to oxidation, and neuronal apoptosis and impairment of synaptic plasticity and, as a result, may be responsible for age-related deficits in the brain (Steen et al. 2005; Bosco et al. 2011).

Abnormal glucose metabolism, such as reduced glucose utilization in the brain, has been reported in early-stage patients with AD and in aged rats (Silverman et al. 2001; Jagust et al. 2006). Glucose can effectively enhance cognition in patients with AD or Down syndrome as well as healthy adults (Korol and Gold 1998; Silverman et al. 2001). Hyperglycemia resulting from insulin deficiency and insulin resistance also contributes to cognitive impairment by increasing oxidative stress, O-linked glycoprotein, and advanced glycation end (Irie et al. 2008). Consequently, preserving the homeostasis of insulin/IGF-1 signaling and/or glucose metabolism may delay the age-related deficits of the brain. In fact, a caloric restriction and physical exercise can promote brain health during aging by enhancing sensitivity to insulin and expression of BDNF (Duan et al. 2001; Komatsu et al. 2008; Ahlskog et al. 2011; Coelho et al. 2013). However, long-term adherence to these lifestyle interventions is difficult for some individuals (Anton et al. 2013). In a recent study, we found that chronic acarbose treatment exerted a protective role against age-related behavioral deficits and changes in biochemical indicators in senescence-accelerated prone mouse P8 (SAMP8, P8) mice (Tong et al. 2015). Acarbose is one of the traditional clinical α-glucosidase inhibitors for the treatment of type 2 diabetes mellitus, but it has common gastrointestinal side effects, such as flatulence, diarrhea, and occasional hepatotoxicity (Van de Laar et al. 2005).

Fortunately, with an antidiabetic mechanism similar to that of acarbose, 1-deoxynojirimycin (DNJ) is much safer and has better efficacy and dose profiles (Kong et al. 2008). DNJ, the main alkaloid component in mulberry leaf, is a potent competitive inhibitor of intestinal α-glycosidases and a new therapeutic agent for diabetes (Kimura et al. 2007). Interestingly, DNJ can be used as a component of functional food. After oral administration, DNJ is quickly absorbed in an intact form from the alimentary tract into the plasma in a dose-dependent fashion and is quickly excreted from the body (Nakagawa et al. 2008). DNJ competitively inhibits a-glucosidase and suppresses glucose absorption, leading to a decrease in the blood glucose level and an increase in insulin sensitivity (Kong et al. 2008; Li et al. 2011).

In addition to its role in modulating glucose metabolism and insulin function, DNJ also has lipid-regulating and antioxidative effects. For example, the administration of a DNJ-rich mulberry extract for 12 weeks can decrease serum levels of triglyceride and very low-density lipoprotein and increase serum level of high-density lipoprotein in patients with hyperlipidemia (Kojima et al. 2010). The suppressive effects on hepatic lipid accumulation and oxidative stress in the liver and plasma have been reported after the intake of DNJ in rodent studies (Kimura et al. 2007; Tsuduki et al. 2013).

In addition, DNJ has an anti-adherence activity and controls the overgrowth of *Streptococcus mutans*, suggesting that it may act as a therapeutic agent in *S. mutans* infection (Islam et al. 2008). DNJ and its derivatives display antiviral activity against bovine viral diarrhea virus, hepatitis B virus, hepatitis C virus, and human immunodeficiency virus (Balzarini 2007; Howe et al. 2013). Moreover, DNJ has been reported to be inhibitory on the metastasis of B16F10 melanoma cells, suggesting an antimetastatic potential (Tsuruoka et al. 1996; Wang et al. 2010a).

Based on these findings, it is of great interest to explore whether DNJ could promote successful brain aging and alleviate the changes in age-related indicators. BDNF is an age-related indicator in the brain that decreases with age (Mattson et al. 2004). It is a key neurotrophic factor that shares similar signaling pathways with insulin and IGFs and plays critical roles in the

regulation of glucose metabolism and cellular stress responses, synaptic plasticity and neurogenesis, and learning and memory (Mattson et al. 2004). Synaptotagmin-1 (Syt-1) and syntaxin-1 (Stx-1) are important neurotransmission-regulating proteins in the presynaptic active zone that we are interested in (Quick 2006; Paddock et al. 2011). The level of Syt-1 in the hippocampus increased with aging and was associated with age-related memory impairment in our previous study using SAMP8 mice (Chen et al. 2007b), whereas Stx-1 was decreased in aged normal rodents and transgenic AD mice (Wirths and Bayer 2010; VanGuilder et al. 2011). In our previous study, chronic acarbose treatment alleviates the age-related Syt-1 increase and Stx-1 decrease in the hippocampus of SAMP8 mice (Tong et al. 2015).

The formation of long-term memory requires transcription and protein synthesis. Epigenetics, especially histone acetylation modifications (HAM), can regulate gene transcription and may be closely related to cognitive ability (Peleg et al. 2010). The fundamental unit of chromatin, the nucleosome, consists of DNA wrap around an octamer of histones H2A, H2B, H3, and H4 (Luger et al. 1997). HAM refers to the addition of acetyl groups to lysine residues of histone by histone acetyltransferase (HAT), while histone deacetylase (HDAC) catalyzes the opposite process. In particular, the acetylation of lysine 8 on H4 (H4K8ac) activates gene transcription and generally favors long-term memory (Lachner et al. 2003).

In this study, we mainly explored whether long-term treatment with DNJ could help promote successful brain aging in a common model for aging, SAMP8 mice, which is a mouse strain with a relatively normal phase of growth and development but early onset and accelerated effects of aging (Takeda 2009). The results reported here are as follows: (i) A battery of behavior tasks was used to evaluate the effect of DNJ on behavioral changes during normal aging. (ii) To explore whether DNJ affects age-related indicators, including the indicators of insulin/IGF-1 and the BDNF system, as well as presynaptic proteins, we determined the serum concentrations of glucose, insulin, BDNF, and IGF-1, as well as the levels of InsR, IGF-1 receptor (IGF-1R), BDNF, and the presynaptic proteins Syt-1 and Stx-1 in the different layers of the dorsal hippocampus. (iii) The level of astrocyte marker glial fibrillary acidic protein (GFAP) in the hippocampus was investigated to explore whether DNJ affects the state of astrocyte activity. (iv) We examined whether DNJ affects the H4K8ac level in the dorsal hippocampus because H4K8 is one of the most studied acetylated histone sites. (v) We analyzed the correlations among the behavioral parameters, the serological data, and the levels of specific proteins in the hippocampus.

Materials and methods

Materials

DNJ was extracted from the fermentation products of *Streptomyces lavendulae* TB-412, a DNJ high-yield strain that was obtained after isolation from the soil and mutated by treatment with ultraviolet light and ethyl sulfate. The DNJ was purified using a macroporous resin and a cation exchange resin followed by a silica resin according to our previously established method (Jang et al. 2012). The purity of DNJ was 23.60 %, which met the requirements of food additives.

Animals and treatments

The SAMP8 mice (8 weeks old, 24–26 g) were purchased from Vital River Laboratory Animal Technology Co., Ltd. (Beijing). The animals were maintained on a 12-h light-dark cycle environment under a controlled temperature (22–25 °C) and humidity (50±5 %) environment with free access to food and water. The animals were randomly divided into an old control group (O-con) and two DNJ groups, with 16 mice (8 males, 8 females) in each group. The mice in the high-dose DNJ (HD-DNJ) and low-dose DNJ (LD-DNJ) groups received water with DNJ dissolved in it (20 and 10 mg/kg/day, respectively) as the sole drinking fluid from 3 to 9 months of age until the start of the behavioral tests. To maintain a constant dose, the concentration of DNJ in the water was adjusted regularly according to water consumption.

General procedures

The body weight of each mouse was monitored monthly from 3 to 9 months old. The mice with movement disorders, hair removal, or any visible tumor were excluded from the experiment. The final number of mice that underwent behavioral tasks and subsequent tests was 12 in the O-con group (6 males, 6 females), 13 in

the HD-DNJ group (6 males, 7 females), and 14 in the LD-DNJ group (7 males, 7 females). In addition, 12 young mice (6 males, 6 females) were added as young controls (Y-con). After a 4-week acclimation period, they undertook the same tests with the other groups at the age of 12 weeks. The battery of tasks was carried out in the following order: episodic-like memory task (ELM; days 1–11), sensorimotor tasks (beam walking and tightrope; day 12), locomotor- and anxiety-based tasks (open field; day 13), novel-object recognition (NOR; days 14–18), novel location recognition (NLR; days 19–23), and Morris water maze task (MWM; days 24–34). All tasks were carried out during the light phase (8–11 a.m. and 2–5 p.m.) and performed in the feeding room to preserve adaptation to the environment. The performances in the memory tasks were recorded with a camera (SONY SSC-DC488P) that was hung above the center of the test apparatuses. All experiments were carried out in accordance with the guidelines for humane treatment set by the Association of Laboratory Animal Sciences and the Center for Laboratory Animal Sciences at Anhui Medical University, with formal approval obtained from the animal subjects review board of Anhui Medical University. All efforts were made to minimize the number of animals used and their suffering.

Behavioral tests

The apparatuses and procedures of the sensorimotor tasks (beam walking, tightrope), open field, NOR, and MWM were described in our previous study (Chen et al. 2011) and are provided in the Supplemental material.

NLR

NLR is a test for spatial memory based on the assumption that rodents with an intact spatial memory could show a naturally exploratory preference for objects in new locations (Murai et al. 2007). On three consecutive days, the mice were habituated individually to a rectangular open-field box (40 cm long×30 cm wide×40 cm high) with no object for 5 min. On the fourth day, the mice were placed in the empty apparatus for a 1-min free exploration before the formal trial. In the sample phase of the formal trial, two identical familiar/sample objects (A1 and A2) were placed in the northern-west (NW) and northern-east (NE) corners of the apparatus and the mice were allowed a 5-min exploration. After a 10-min delay (10-min phase), object A2 in the NE corner was moved to the southern-east (SE) corner and the mice were placed in the box for a 5-min trial (as depicted in Fig. 1a). After a 24-h delay (24-h phase), object A2 was moved to the center of the box and the mice were reintroduced for a 5-min trial. It was considered exploration if an animal touched the object with its vibrissae, snout, or forepaws. For each trial, the exploring total time (Tt) and the time spent exploring the novel location (Tn) objects within the first 1 min during the choice phases were recorded by analyzing the video using software (XNote Stopwatch 1.39). The preferential index (PI) for a novel location in the choice phases was defined as Tn/Tt×100 %.

ELM

The apparatus was a rectangle metal open-field box (30 cm×30 cm×40 cm) with a black floor and walls, surrounded with a black curtain to prevent mice from looking out (Dere et al. 2005). A round hole (diameter 0.5 cm) was drilled into the west and east walls at a height of 30 cm, possibly serving as visual cues. The mice were released into the center of the apparatus for a 1-min exploration for seven consecutive days. On days 8–10, the mice were familiarized daily with the apparatus with no object for 5 min. On the following 2 days, the mice received three daily sessions of 10-min acclimations with at least a 30-min interval in the apparatus in which two objects (A1, A2) were placed into the far corners (the NW and NE). On day 13, each mouse received two sample trials and a test trial. In the first sample trial, four copies of a novel object (B) were arranged in a triangle-shaped spatial configuration, one in the center of the northern wall (NC), one in the center of the southern wall (SC), one in the southern-west (SW) corner, and one in the southern-east (SE) corner (as depicted in Fig. 1b). The mice were placed into the field and allowed a 10-min exploration. After a 50-min delay, the mice received the second sample trial, when four objects (B) were removed and four novel objects (C) were placed in the four corners of the open field. After a delay of 50 min, in the test trial, two copies of object B ("old familiar" objects) from sample trial 1 were placed in the NE and SW corners and two objects C ("recent familiar" objects) from sample trial 2 were placed in the NW and SE corners. The mice were reintroduced to the apparatus for a 10-min trial. The object B in the NE corner is the displaced "old familiar"

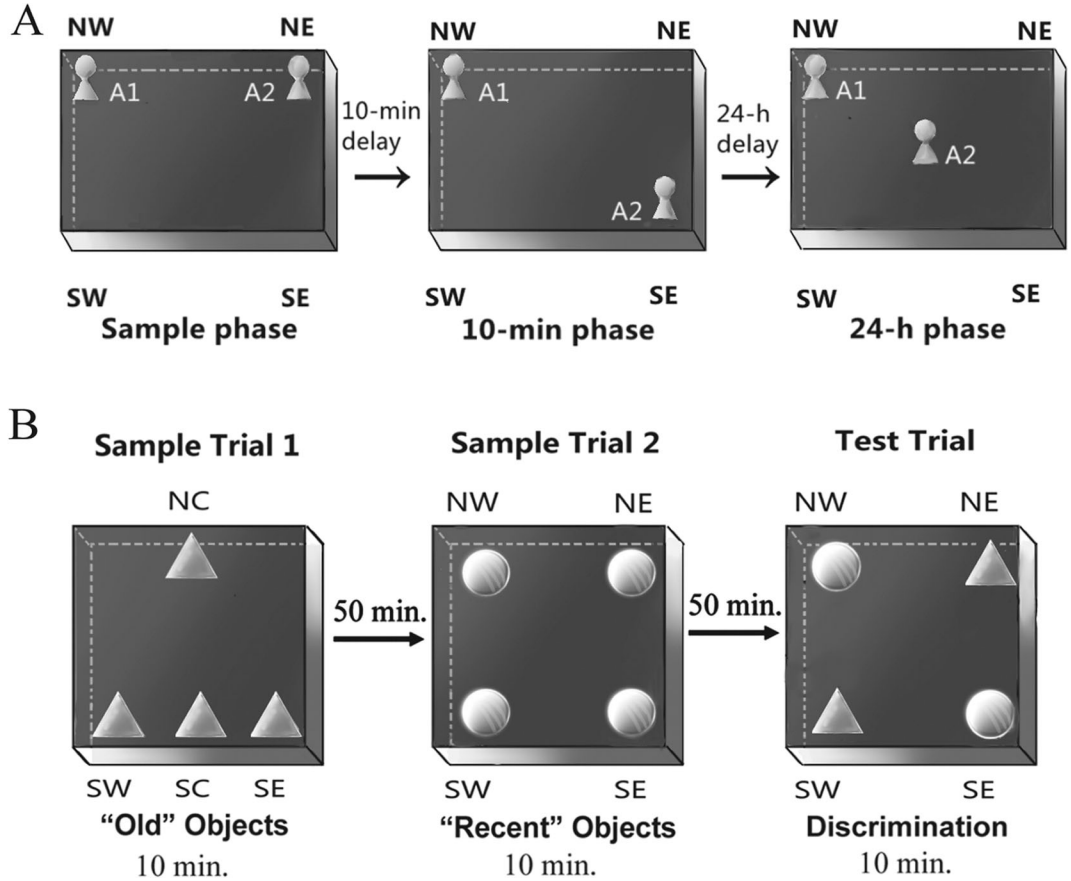

Fig. 1 Schematic drawing of the protocol in two memory tasks. **a** In the novel location recognition, two identical sample objects (A_1, A_2) were placed in the north-west (NW) and north-east (NE) corners of the box in the sample phase. In the 10-min phase and the 24-h phase, one of the sample objects (A_2) was moved to a novel location. **b** For the episodic-like memory task, during the first and second sample trials, the objects were arranged as the figure shows. In the test trial, two objects B (old objects from the first sample trial) were placed in the south-west (old stationary object) and NE corner (old displaced object). Two recent objects C were placed in the other two corners

object, i.e., the least recently seen object that had moved location. After each trial, the apparatus and objects were thoroughly cleaned with water. The definition of the exploration was identical to that in the NLR. The time spent exploring each object was recorded by software (XNote Stopwatch 1.39) based on the videos. The PI for the old object (PIo) was defined as time spent exploring the "old familiar" object (To) / total exploration time for all four objects (Tt). The PI for the displaced "old familiar" object (PIod) was defined as the time spent exploring the displaced "old familiar" objects / To (Dere et al. 2005).

Preparation of serum and tissue samples

To avoid the effects of the behavioral tests on biochemical indicators, the mice were anesthetized with halothane and killed 15 days after the behavioral tests. The blood samples were collected after quickly removing the eyeball from the socket. Serum was obtained after centrifugation and quickly frozen at −80 °C until use. After decapitation, the brains were rapidly removed and bisected in the mid-sagittal plane, fixed in 4 % paraformaldehyde at 4 °C for 3 days, and paraffin-embedded for immunohistochemistry. Coronal sections were cut at a 6-μm thickness from tissue paraffin blocks by a microtome.

Serum biochemical analyses

Serum concentrations of glucose, insulin, BDNF, and IGF-1 were detected using an enzyme-linked immunosorbent assay (ELISA). ELISA kits for glucose and insulin (Beyotime Institute of Biotechnology, China)

and BDNF and IGF-1 (Shanghai Yuanye Biological Technology Co., China) were used according to the manufacturer's instructions. The samples (10 μl) and sample dilutions (40 μl) were added to the precoated plate and incubated at 37 °C for 30 min. Then, the precoated plate was washed and 50 μl of HRP-conjugated reagent was added and incubated at 37 °C for 30 min. After washing, chromogen was added and the mixture was incubated at 37 °C for 15 min. The optical density (OD) was measured spectrophotometrically at 450 nm. The glucose or protein content was quantified by comparing the OD of the samples to the standard curve.

Immunohistochemistry

The streptavidin-biotin-peroxidase complex (SABC) method was applied as described (Nagashima et al. 1992). Antigen retrieval was performed by microwave heating for 10 min in sodium citrate solution (0.01 mol/l, pH 6.0). Nonspecific reactions were blocked with 0.4 % Triton X-100, H_2O_2, and 5 % bovine serum albumin prior to incubation with primary antibodies overnight at 4 °C. The primary antibodies included rabbit polyclonal anti-InsR (1:50), IGF-1R (1:50), BDNF (1:100), Syt-1 (1:400), Stx-1 (1:400), GFAP (1:400), and H4K8ac (1:1000), all of which were purchased from Abcam (Cambridge, MA, USA). The following day, the sections were washed with phosphate buffered saline and incubated with a biotin-labeled secondary antibody and SABC (Wuhan Boster Bioengineering Limited Co., China) and then visualized by diaminobenzidine. Two sections from each animal were stained for each protein.

An optical microscope (Olympus, Japan) equipped with a digital camera (Nikon, Japan) was used to take digital photographs of the stained sections. To reveal the changes in the protein levels, we analyzed proteins in each layer in the subregions of the hippocampus. After pictures of the complete hippocampus were obtained at low magnification (×4) for general observation, the images for analysis were taken in high magnification (×20) in the following order: hilus (HL), granule cell layer (GL), and molecular layer (ML) of the DG; ML, radiation layer (RL), pyramidal cell layer (PL), and original layer (OL) of the CA1 subregion; and ML, stratum lucidum (SL), PL, and OL of the CA3 subregion. The average optical density (AOD) of immunoreactivity in each layer of the hippocampus was measured using Image-Pro Plus 6.0 image software following the semiquantitative method introduced by Xavier et al. (2005). Briefly, the intensity calibration function was activated for the subtraction of background staining prior to analysis. For the images of each sample, the intensity of the background staining was measured and the mean value was used for the incident light calibration to minimize the effect of background staining. In each layer in the hippocampal subregions, the areas of interest (AOIs) were selected randomly and the optical density values of immunoreactive products were measured. The AOD in each layer was obtained by calculating the average value of the mean optical density (optical density/AOI) in different AOIs and represented the relative level of the specific protein.

Statistical analysis

The results are expressed as the mean±SEM for the parametric data. Repeated measures analysis of variance (rm-ANOVA) was used to analyze the body weight data and the place navigation trial in the MWM. For parametric data in other tests, the analysis was performed using two-way ANOVA with group and sex as independent variants. Dunnett's post hoc test was used with the O-con as the control, and the Bonferroni post hoc test was used to reveal any difference between the two DNJ groups. In the NOR, NLR, and ELM tasks, one-sample *t* test was used to analyze whether the PIs in each group were different from chance performance (50 %), followed by the analysis of age and DNJ effect by two-way ANOVA. Canonical correlation analysis was used to analyze the correlations between cognitive performance and biochemical indicators. All analyses were conducted using SPSS 13.0 for Windows. Significance was assumed when $P<0.05$.

Results

Body weight

The rm-ANOVA results indicated that the DNJ treatment had no significant effect on body weight [$F_{(2,\ 37)}=0.128$, $P=0.881$]. The females had lower body weights than the males [$F_{(1,\ 38)}=122.057$, $P<0.001$] in each group (Ps<0.001), as shown in Electronic supplementary Table 1.

Behavioral tests

Sensorimotor behaviors

Beam walking The two-way ANOVA results (Table 1) showed significant group and sex effects on the balance time [$F_{(3,\ 48)}$=6.259, P=0.001; $F_{(1,\ 50)}$=40.58, P<0.001, respectively]. Further analysis showed that the O-con exhibited a significantly shorter balance time than the Y-con (P=0.003) in both the males (P=0.032) and females (P=0.033). The HD-DNJ mice had a longer balance time than the O-con (P=0.029) and the LD-DNJ mice (P=0.041). The LD-DNJ mice had a similar balance time with the O-con (P>0.05). The males exhibited a shorter balance time than the females in the O-con and each of the DNJ groups (Ps<0.05). Sex had no significant effect in the Y-con (P>0.05).

Tightrope The group effect was significant on the suspension time [$F_{(3,\ 48)}$=4.942, P=0.005] and on the tightrope score [$F_{(3,\ 48)}$=6.080, P=0.002] (Table 1). Further analysis showed that compared to the Y-con, the O-con exhibited a significantly shorter suspension time (P=0.006) for both the males and females (Ps< 0.05) and a lower tightrope score (P<0.001), mainly in the males (P=0.014). Compared to the O-con, the HD-DNJ mice exhibited a longer suspension time (P= 0.005), mainly attributable to the males (P=0.011), and a higher tightrope score (P=0.025). The LD-DNJ mice also exhibited a longer suspension time than the O-con (P=0.019), mainly attributable to the males (P= 0.015). The tightrope score of the LD-DNJ mice was similar to that of the O-con (P=0.148). For all mice combined, the males exhibited a shorter suspension time than the females [$F_{(1,\ 50)}$=4.599, P=0.038], but the sex effect was not significant when each group was analyzed separately. Sex had no significant effect on the tightrope score (P>0.05).

Locomotor- and anxiety-based tasks

Open field The group exerted a significant effect on the latency left from the first square [$F_{(3,\ 48)}$=3.413, P= 0.026] and the number of squares crossed [$F_{(3,\ 48)}$=11.589, P<0.001], but not the peripheral time [$F_{(3,\ 48)}$=1.507, P= 0.227] (Table 1). Dunnett's test showed that the O-con exhibited a shorter latency (P=0.016), fewer squares crossed than the Y-con (P =0.003), and a similar number of squares crossed to the two DNJ groups (Ps>0.05). The HD-DNJ mice exhibited a longer latency than the O-con (P=0.045). The LD-DNJ mice showed a similar performance to the O-con (Ps>0.05). The two DNJ groups were not significantly different (Ps>0.05). Sex and the interaction of group × sex did not have a significant effect on the open-field performance (Ps>0.05).

Performance of cognitive tests

Morris water maze

Place learning The rm-ANOVA results revealed a significant group effect on the swimming velocity [$F_{(3,\ 47)}$=27.110, P<0.001] and distance [$F_{(3,\ 47)}$=7.962, P<0.001]. The O-con had a significantly lower velocity than the Y-con (P<0.001) and a similar velocity with the DNJ-treated mice (Ps>0.05; see Fig. 2a). Therefore, the swimming distance before locating the platform was considered as the indicator of spatial learning. The distance progressively decreased daily for all mice combined [$F_{(9,\ 450)}$=10.052, P<0.001], suggesting that the mice were able to learn this task. The O-con showed a significantly longer distance than the Y-con (P<0.001;

Table 1 Performance of the SAMP8 mice in the sensorimotor task and locomotor- and anxiety-based tasks

Tasks	Parameters	Old control	Young control	HD-DNJ group	LD-DNJ group
Beam walking	Balance time (s)	91.5±10.2	136.2±10.3*	129.6±9.2*	90.5±13.3
Tightrope	Suspension time (s)	44.2±3.4	56.2±1.8*	55.1±1.9*	53.4±2.3*
	Tightrope score	53.9±3.5	86.3±4.2*	77.6±5.7*	68.4±7.0
Open field	Latency (s)	6.36±0.7	11.7±1.7*	10.8±1.3*	8.5±1.0
	Number of squares crossed	123.6±6.5	159.3±9.7*	121.4±6.0	106.6±7.0
	Peripheral time (s)	230.9±10.2	261.0±7.6*	237.3±12.0	228.9±10.9

The results were expressed as mean±SEM

*P<0.05 denotes significant difference compared to the old controls

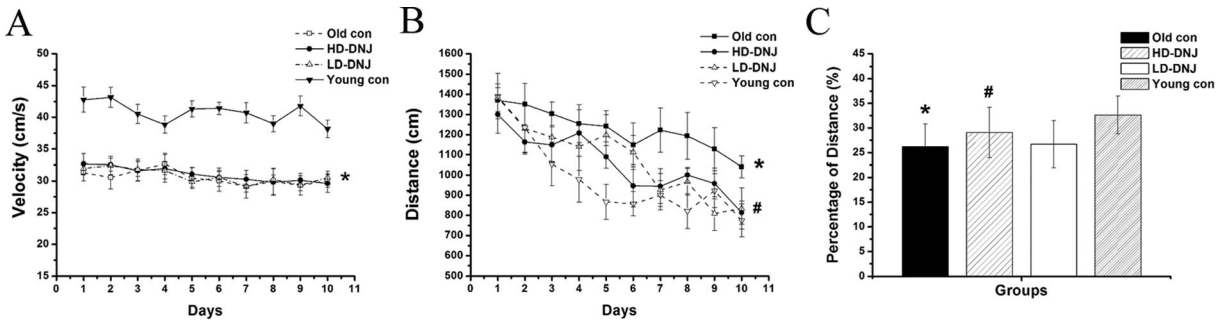

Fig. 2 Performance of the SAMP8 mice in the MWM. The old controls exhibited a significantly lower swimming velocity (**a**) and longer distance (**b**) than the young mice in the place-learning phase and a lower percentage of distance (**c**) than the young mice in the target quadrant in the probe trial. Both the HD-DNJ and the LD-DNJ mice had shorter distances than the O-con (**b**). The HD-DNJ mice, but not the LD-DNJ mice, showed a higher percentage of distance (**c**) than the O-con. The *bars* represent SEM. *$P<0.05$ denotes significant DNJ effect. #$P<0.05$ denotes significant age effect

see Fig. 2b). Both the HD-DNJ and the LD-DNJ mice had a shorter distance than the O-con ($P=0.004$ and 0.008, respectively). Sex and the interaction of group × sex, group × day, sex × day, and group × sex × day had no significant effect on the performance in the trials (Ps>0.05).

Probe trial The group effect was significant on the percentage of distance in the target quadrant where the platform was placed during the place learning trial [$F_{(3, 47)}=3.606$, $P=0.021$]. Further analysis showed that the O-con exhibited a significantly lower percentage of swimming distance in the target quadrant than the Y-con ($P=0.012$). The HD-DNJ treatment alleviated this age-related alteration ($P=0.040$; Fig. 2c). The LD-DNJ mice performed similarly to the O-con ($P>0.05$). Neither sex nor interactions of group × sex had a significant effect on the percentage of distance (Ps>0.05).

NOR

During the sample phase, the mice in all of the groups spent equal amounts of time exploring either of the two identical objects, indicating no biased exploratory preference. In the 10-min phase, the ANOVA results revealed significant differences in the Tt [$F_{(3, 48)}=22.333$, $P<0.001$] and PI [$F_{(3, 48)}=12.211$, $P<0.001$] among the four groups. The O-con exhibited lower Tt and PI than the Y-con (Ps<0.001). Both the HD- and LD-DNJ mice had higher PIs than the O-con (Ps<0.001). In the 24-h phase, the group effect was significant on the Tt [$F_{(3, 48)}=29.656$, $P<0.001$], but not on the PI [$F_{(3, 48)}=1.981$, $P=0.321$] (Table 2). The O-con exhibited a lower Tt than the Y-con ($P<0.001$). Sex and group × sex had no significant effect on the performance in both choice phases (Ps>0.05).

NLR

During the sample phase, the mice in all of the groups had equivalent exploration preferences for both objects. In the 10-min phase, the group effect on the Tt [$F_{(3, 48)}=4.611$, $P=0.007$] and PI [$F_{(3, 48)}=13.067$, $P<0.001$] was significant. The O-con exhibited significantly lower Tt and PI than the Y-con ($P=0.021$; $P<0.001$). The HD- and LD-DNJ mice exhibited significantly higher PIs than the O-con (Ps<0.001; see Table 2). In the 24-h phase, no significant difference in the Tt and PI was observed among the groups (Ps>0.05). Sex and group × sex had no significant effect on the NLR performances (Ps>0.05).

ELM

The Tt, PIo (the PI for old object), and PIod (the PI for old displaced objects) of each group are presented in Table 2. The PIo and PIod in the Y-con and the two DNJ groups were significantly higher than 50 % (Ps<0.05), suggesting a preferential exploration of the displaced "old familiar" object when compared to the stationary "old familiar" object and a preferential exploration of the "old familiar" object compared to the "recent familiar" object. However, the PIo and PIod in the O-con showed no significant difference with 50 % ($P>0.05$). The group effects on the Tt, PIo, and PIod were significant [$F_{(3, 48)}=104.25$, $P<0.001$; $F_{(3, 48)}=54.604$, $P<0.001$; $F_{(3, 48)}=3.753$, $P=0.018$, respectively]. The O-con had a lower Tt ($P<0.001$), PIo ($P<0.001$), and PIod ($P=0.006$) than the Y-con, indicating an age-related deficit of episodic memory. The HD-

Table 2 Performances of the SAMP8 mice in the memory tasks

Tasks	Phases	Parameters	Old control	Young control	HD-DNJ group	LD-DNJ group
Novel object recognition	10-min phase	Tt (s)	7.7±0.6	13.0±1.4*	6.7±0.3	7.6±0.6
		PI (%)	49.2±2.6	62.6±1.1*	65.8±3.0*	63.2±3.4*
	24-h phase	Tt (s)	6.4±0.3	12.2±1.0*	7.2±0.4	7.2±0.3
		PI (%)	48.5±3.1	47.4±1.7	52.7±3.2	51.6±3.1
Novel location recognition	10-min phase	Tt (s)	5.7±0.5	8.3±0.6*	5.9±1.3	5.6±0.8
		PI (%)	51.0±3.7	63.9±2.8*	63.7±3.4*	61.1±5.1*
	24-h phase	Tt (s)	5.2±0.6	6.7±0.5	5.1±0.5	4.5±0.4
		PI (%)	51.6±4.2	57.5±3.1	54.7±4.7	51.1±4.3
Episodic-like memory		Tt (s)	23.1±0.6	38.3±0.7*	30.0±1.0*	36.2±1.6*
		PIo (%)	50.4±0.8	59.6±0.7*	55.5±0.8*	56.4±1.0*
		PIod (%)	49.6±2.8	57.8±0.8*	55.9±0.8*	54.8±0.4*

Data are expressed as mean±SEM

PI preference index for novel object in the NOR or for novel location in the NLR, *PIo* preference index for old objects, *PIod* preference index for displaced old object, *Tt* total exploring time

*$P<0.05$ denotes significant difference compared to the old controls

DNJ mice had a higher Tt ($P<0.001$), PIo ($P<0.001$), and PIod ($P=0.017$) than the O-con. The LD-DNJ group also showed higher Tt ($P<0.001$), PIo ($P<0.001$), and PIod ($P=0.046$) than the O-con. Sex and the interaction of group × sex had no significant effect on the ELM performance (Ps>0.05).

Serum concentration of glucose, insulin, IGF-1, and BDNF

The group effect was significant on the serum levels of insulin [$F_{(3,\ 48)}=14.004$, $P<0.001$], IGF-1 [$F_{(3,\ 48)}=34.065$, $P<0.001$], and BDNF [$F_{(3,\ 48)}=16.188$, $P<0.001$], but insignificant on the serum glucose [$F_{(3,\ 48)}=1.928$, $P=0.139$] (Table 3). Further analysis showed that the O-con exhibited a lower insulin level than the Y-con ($P=0.001$) and similar IGF-1 and BDNF levels to the Y-con (Ps>0.05). Both the HD- and LD-DNJ mice showed significantly higher levels of insulin ($P=0.002$; $P=0.024$), IGF-1 ($P=0.005$; $P=0.034$), and BDNF ($P=0.005$; $P=0.034$) than the O-con. Neither sex nor group × sex had significant effects on the serological assays (Ps>0.05).

Immunohistochemistry

Levels of InsR, IGF-1R, and BDNF

Compared to the Y-con (Table 4), the O-con showed lower levels of InsR (Fig. 3) in all layers of the hippocampal subregions and BDNF (Fig. 4) in the DG-GL, DG-ML, CA1-PL, CA3-SL, and CA3-PL and higher levels of IGF-1R (Fig. 5) in all layers, except for DG-GL, CA1-PL, and CA3-PL (Ps<0.05). Compared to the O-con, the HD-DNJ mice had higher levels of InsR in the CA1 (ML, PL, and OL) and CA3 (ML and OL) and BDNF in the DG-GL, DG-ML, CA1-PL, and CA3-PL and lower levels of IGF-1R in the DG-HL and CA1-RL (Ps<0.05). However, the LD-DNJ mice only had higher levels of BDNF in the DG-GL and CA1-PL and a lower level of IGF-1R in the CA3-OL (Ps<0.05). Between the DNJ groups, the HD-DNJ mice only had significantly higher InsR in the CA1-ML and CA3-OL (Ps<0.05).

Contents of Syt-1 and Stx-1

The O-con showed significantly increased Syt-1 in all layers of the different hippocampal subregions, except for the DG-HL, than the Y-con (Ps<0.01, Fig. 6), but reduced Stx-1 in the DG-HL, CA1-RL, CA1-PL, CA1-OL, and CA3-ML (Ps<0.05, Fig. 7) (see Table 4). Compared to the O-con, the HD-DNJ mice showed a significantly decreased Syt-1 in all layers, except for DG-HL, and an increased Stx-1 in the DG-HL, CA1-RL, and CA3-ML (Ps<0.05). In addition, the LD-DNJ mice showed significantly lower Syt-1 levels in the DG-GL, DG-ML, CA1-ML, CA1-

Table 3 Serum concentrations of glucose, insulin, IGF-1, and BDNF in the SAMP8 mice

Groups	Glucose (mmol/l)	Insulin (mIU/l)	IGF-1 (ng/ml)	BDNF (pg/ml)
Old control	8.6±0.4	10.0±0.4	57.6±2.0	1228.5±30.6
Young control	8.3±0.5	13.7±0.7*	57.1±1.4	1209.1±26.5
HD-DNJ group	8.1±0.6	13.0±0.7*	69.4±1.5*	1433.0±51.2*
LD-DNJ group	8.5±0.7	11.8±0.5*	67.5±3.1*	1417.1±46.4*

Data are expressed as mean±SEM

*$P<0.05$ denotes significant difference compared to the old controls

PL, CA3-ML, and CA3-PL and higher levels of Stx-1 in the DG-HL (Ps<0.05).

Level of GFAP

The O-con had higher GFAP immunoreactivity in all layers, besides the CA1-OL and CA3-PL, than the Y-con (Ps<0.05; see Table 4). The GFAP-positive astrocytes in the aged hippocampus were morphologically enlarged (Fig. 8). Compared to the O-con, the HD-DNJ mice showed lower levels of GFAP in the DG-ML, all CA1 layers, CA3-ML, and CA3-OL (Ps<0.05); and the LD-DNJ mice had lower levels of GFAP in the DG-GL, DG-ML, CA1-ML, and CA3-ML (Ps<0.05). There was no significant difference in GFAP level between the DNJ groups (P<0.05).

Level of H4K8ac

The histones are located within the cell nuclei; therefore, only the layers that contain the cell bodies of dentate granule cells or pyramidal neurons were analyzed (Fig. 9). Compared to the Y-con, the O-con displayed significantly lower levels of H4K8ac in the DG-GL, CA1-PL, and CA3-PL (Ps<0.05). The HD-DNJ mice in the DG-GL, CA1-PL, and CA3-PL and the LD-DNJ mice in the CA3-PL had higher levels of H4K8ac than the O-con (Ps<0.05). The HD-DNJ mice had significantly higher H4K8ac levels in all three subareas than the LD-DNJ mice (Ps<0.05).

Correlations between cognitive performances and the results of the serum and immunohistochemical assays

For the serological tests, the serum level of insulin was positively correlated with the PI in the NLR task and the PIo and PIod in the ELM task. The serum levels of BDNF and IGF-1 were positively correlated with the PI in the NOR (see Table 5). For each hippocampal protein, the correlation coefficients between protein levels in the hippocampal layers and memory performances are shown in Table 6 and Electronic supplementary Tables 2 to 7, respectively. The correlations were analyzed for all the mice combined and then for mice in separately groups. For all the mice combined, the InsR and Stx-1 levels correlated positively with the percentage of distance in the target quadrant in the MWM, the PIs in the NOR and NLR, and the PIo and PIod in the ELM (see Table 6 and Electronic supplementary Table 5). The InsR levels in most hippocampal layers correlated negatively with the swimming distance in the MWM. The IGF-1R levels in several hippocampal layers correlated positively with the swimming distance in the MWM and negatively with the PIs in the NOR and NLR and the PIo in the ELM. Negative correlations between IGF-1R level and the target-quadrant distance percentage in the MWM and the PIod in the ELM were only found in the DG-HL region (see Electronic supplementary Table 2). The BDNF level correlated negatively with the swimming distance in the MWM and positively with the PI in the NLR and the PIo in the ELM (see Electronic supplementary Table 3). The Syt-1 level correlated negatively with learning and memory ability in the MWM and with the PIs in the other memory tasks, especially the PI in the NLR and the PIo in the ELM (see Electronic supplementary Table 4). The GFAP levels in hippocampal layers negatively correlated with the memory indexes in all tasks, especially with those in the ELM task (see Electronic supplementary Table 6). The H4K8ac level in all cell layers correlated with the swimming distance in the MWM negatively and with the PIs in the NLR and ELM positively. The H4K8ac level in the CA3-PL positively correlated with the PI in the NOR (see Electronic supplementary Table 7). When mice in each

Table 4 The relative protein levels of InsR, IGF-1R, BDNF, Syt-1, and Stx-1 indicated by AOD of immunohistochemical staining (×100)

Proteins	Groups	DG			CA1				CA3			
		HL	GL	ML	ML	RL	PL	OL	ML	SL	PL	OL
InsR	O-con	2.17±0.33	4.66±0.83	2.06±0.42	3.15±0.61	1.72±0.44	4.60±0.76	2.65±0.60	1.90±0.48	3.24±0.71	6.20±0.51	3.33±0.42
	Y-con	4.88±0.43**	8.62±0.76**	4.12±0.51**	6.07±0.66*	4.72±0.53**	8.18±0.75**	5.90±0.67**	4.77±0.57**	5.43±0.51**	8.56±0.36**	6.28±0.45**
	HD-DNJ	3.26±0.37	6.41±0.51	2.92±0.39	5.90±0.47*	2.99±0.50	7.05±0.57 *	4.25±0.58*	3.34±0.43*	3.69±0.44	6.29±0.65	4.79±0.38*
	LD-DNJ	2.86±0.49	5.44±0.93	2.19±0.32	3.85±0.51	2.11±0.38	6.03±0.59	3.44±0.56	2.56±0.51	2.76±0.66	5.70±0.65	3.02±0.43
IGF-1R	O-con	2.65±0.32	3.00±0.34	2.65±0.32	3.11±0.59	2.75±0.51	4.29±0.74	3.99±0.84	1.81±0.45	2.61±0.46	4.52±0.71	2.31±0.44
	Y-con	0.99±0.41*	1.59±0.74	1.06±0.39*	1.31±0.33*	0.47±0.19**	2.67±0.57	0.84±0.31**	0.61±0.11*	1.22±0.19*	3.87±0.66	1.09±0.22*
	HD-DNJ	1.48±0.41*	2.09±0.45	2.04±0.45	2.41±0.46	1.32±0.40*	3.71±0.61	2.46±0.47	1.12±0.30	1.76±0.41	3.28±0.61	1.46±0.26
	LD-DNJ	1.82±0.62	2.29±0.68	1.86±0.50	2.26±0.52	1.75±0.46	4.26±0.59	2.51±0.54	1.31±0.55	1.81±0.39	3.93±0.59	1.28±0.38*
BDNF	O-con	3.04±0.34	2.26±0.40	2.55±0.36	3.88±0.54	3.16±0.52	3.24±0.41	2.23±0.34	2.52±0.45	3.64±0.44	4.77±0.56	3.35±0.48
	Y-con	4.22±0.64	5.25±0.69**	4.40±0.64*	5.37±0.56	5.05±0.66	5.65±0.52**	3.78±0.57	3.72±0.60	5.29±0.54*	7.62±0.49**	4.93±0.59
	HD-DNJ	3.70±0.77	5.83±1.04**	4.59±0.84*	5.28±0.78	4.81±0.78	6.24±0.70**	3.82±0.62	3.69±0.69	5.34±0.84	6.87±0.66*	5.20±1.22
	LD-DNJ	3.64±0.71	5.06±1.05*	3.96±0.68	4.15±0.79	3.40±0.54	5.08±0.78*	3.07±0.71	2.80±0.69	3.47±0.70	5.24±0.76	3.20±0.77
Syt-1	O-con	7.03±1.48	1.32±032	3.53±0.82	3.16±0.81	6.65±1.22	2.15±0.41	6.30±1.17	4.24±0.76	4.92±0.54	2.58±0.51	5.30±0.83
	Y-con	4.11±1.15	0.16±0.08**	0.95±0.15**	0.53±0.05**	1.07±0.31**	0.27±0.07**	1.06±0.23**	0.89±0.20**	1.08±0.26**	0.31±0.10**	1.29±0.22**
	HD-DNJ	4.53±0.92	0.17±0.06*	0.96±0.18*	0.58±0.26*	2.49±0.67*	0.50±0.16*	2.57±0.95*	1.05±0.43*	1.75±0.51*	0.68±0.13*	1.94±0.61*
	LD-DNJ	6.92±1.01	0.49±0.10*	2.10±0.18*	1.64±0.36*	4.63±0.77	0.78±0.16*	5.03±0.80	1.88±0.40*	3.85±0.89	1.27±0.34*	3.70±0.48
Stx-1	O-con	0.88±0.06	0.15±0.05	0.42±0.12	0.34±0.11	0.45±0.11	0.03±0.00	0.25±0.08	0.24±0.08	0.63±0.08	0.03±0.00	0.47±0.15
	Y-con	1.76±0.14*	0.33±0.12	0.57±0.19	0.68±0.18	1.40±0.22**	0.13±0.05*	0.67±0.19*	0.77±0.21*	1.17±0.21	0.05±0.01	0.75±0.20
	HD-DNJ	1.41±0.19*	0.11±0.05	0. 56±0.18	0.56±0.22	1.22±0.14*	0.06±0.02	0.34±0.13	0.56±0.10*	1.14±0.22	0.03±0.01	0.72±0.18
	LD-DNJ	1.32±0.16*	0.07±0.01	0.32±0.09	0.37±0.08	0.66±0.09	0.04±0.01	0.22±0.06	0.28±0.08	0.75±0.14	0.02±0.01	0.52±0.04
GFAP	O-con	2.72±0.60	1.47±0.39	2.30±0.43	3.54±0.74	2.01±0.46	1.44±0.48	1.95±0.28	1.92±0.59	1.37±0.35	0.35±0.08	2.09±0.60
	Y-con	1.12±0.39*	0.48±0.15*	0.59±0.22**	1.46±0.55*	0.92±0.20*	0.25±0.06*	1.31±0.32	0.78±0.20*	0.50±0.14*	0.25±0.08	0.69±0.11*
	HD-DNJ	1.31±0.21	0.76±0.22	0.86±0.15*	0.93±0.20**	0.95±0.12*	0.29±0.06*	0.99±0.12*	0.70±0.17*	0.62±0.14	0.39±0.10	0.54±0.09*
	LD-DNJ	1.14±0.15*	1.15±0.15	1.02±0.26*	0.90±0.13**	1.13±0.15	0.49±0.10	1.22±0.25	0.79±0.12*	0.71±0.17	0.41±0.08	1.06±0.23
H4K8ac	O-con	–	2.04±0.08	–	–	–	1.76±0.09	–	–	–	1.34±0.09	–
	Y-con	–	3.85±0.09**	–	–	–	2.86±0.10**	–	–	–	2.84±0.10**	–
	HD-DNJ	–	3.19±0.09**	–	–	–	2.65±0.08**	–	–	–	2.58±0.11**	–
	LD-DNJ	–	2.10±0.10	–	–	–	2.01±0.08	–	–	–	1.62±0.08*	–

Data are expressed as mean±SEM

DG dentate gyrus, *HL* Hilus, *GL* granule cell layer, *ML* molecular layer, *RL* radiation layer, *PL* pyramidal cell layer, *OL* original layer, *SL* stratum lucidum, *O-con* old controls, *Y-con* young controls

*$P<0.05$, **$P<0.01$ denote significant difference compared to the old controls

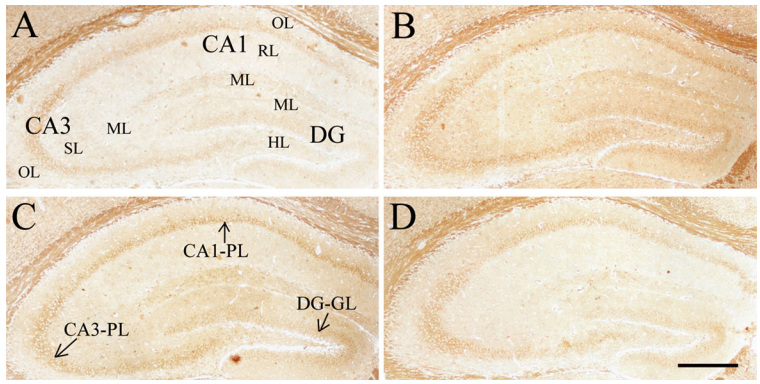

Fig. 3 Effect of age or DNJ on insulin receptor (InsR) immunohistochemical staining in the dorsal hippocampus of the SAMP8 mice. Representative low-magnification photos in the O-con (**a**), Y-con (**b**), HD-DNJ (**c**), and LD-DNJ (**d**) groups are shown. The InsRs were densely expressed in the layers containing cell bodies, i.e., DG-GL, CA1-PL, and CA3-PL. The old controls had lower InsR immunoreactivity than the young controls, which was alleviated by the HD-DNJ treatment. *DG* dentate gyrus, *GL* granule cell layer, *PL* pyramidal cell layer. *Scale bar*=400 μm

group were analyzed separately, much less significant correlations between the proteins levels and the cognitive performances could be observed, which may due to the small sample size.

Before the canonical correlation analysis, the correlations between the levels of each protein in all hippocampal layers were analyzed. The protein levels in the different hippocampal layers had strong correlations, which were not fitted for canonical correlation analysis. Thus, the average level of each protein in all layers of the hippocampus for each mouse was calculated for the subsequent canonical correlation analyses.

We analyzed the canonical correlation between the seven indicators of the insulin/IGF-1 and BDNF system (including serum glucose, insulin, BDNF, and IGF-1 and the hippocampal IGF-1R, InsR, and BDNF) and memory test performance (including the swimming distance and the percentage of distance in the target quadrant in the MWM, the PIo and PIod in the ELM, and the PIs in the NOR and NLR). The first correlation was statistically significant (r=0.852, F=42.0, P=0.001, redundancy index=0.184), indicating a close association between these biochemical indicators and memory performance. The loadings and cross loadings of the variables for the first canonical correlation are presented in Table 7. The loadings of the variables for the insulin/IGF-1 and BDNF system indicated that IGF-1R and InsR contributed most to the first correlation. The

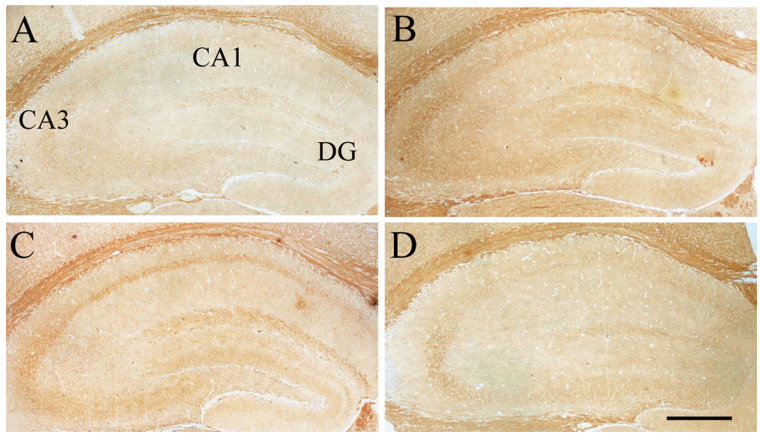

Fig. 4 Effect of age or DNJ on BDNF immunohistochemical staining in the dorsal hippocampus. Representative low-magnification photos in the O-con (**a**), Y-con (**b**), HD-DNJ (**c**), and LD-DNJ (**d**) groups are shown. For the Y-con, BDNF immunoreaction was detected in all of the layers, especially in the CA1-PL, CA3-SL, and CA3-PL. The analysis of average optical density showed that the O-con had a lower BDNF level in several layers than the young controls. DNJ alleviated the decrease in BDNF level in the old SAMP8 mice. *PL* pyramidal cell layer, *SL* stratum lucidum. *Scale bar*=400 μm

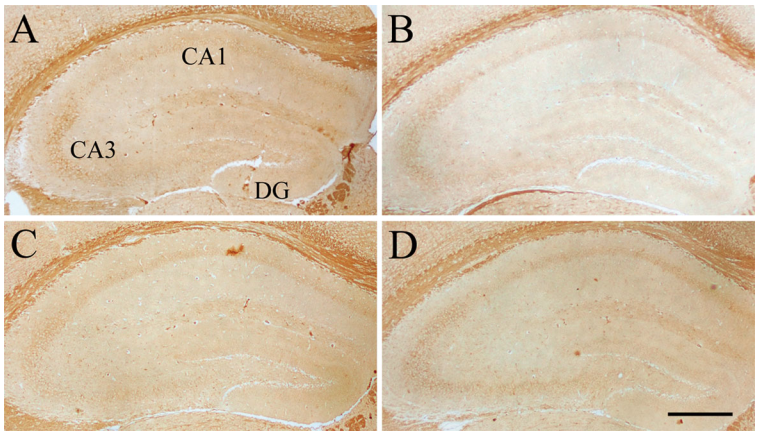

Fig. 5 Effect of age or DNJ on IGF-1R immunohistochemical staining in the dorsal hippocampus. Representative low-magnification photos in the O-con (**a**), Y-con (**b**), HD-DNJ (**c**), and LD-DNJ (**d**) groups are shown. An IGF-1R immunoreaction was detected in all layers of the O-con. For the Y-con, an IGF-1R immunoreaction was mainly detected in the DG-GL, CA1-PL, and CA3-PL. The analysis of average optical density showed that DNJ decreased the elevated IGF-1R level in the old controls. *DG* dentate gyrus, *GL* granule cell layer, *PL* pyramidal cell layer. *Scale bar*=400 μm

loadings of the memory indicators demonstrated that the swimming distance in the MWM and the PI in the NOR contributed most to the first correlation.

Then, we analyzed the canonical correlation between the four age-related indicators (Syt-1, Stx-1, GFAP, and H4K8ac) and the indicators of cognitive performance mentioned above. The first canonical correlation was significant (r=0.842, F=24.0, P=0.001, redundancy index=0.530). The loadings of the age-related indicators in the hippocampus suggested that they were all strongly correlated with cognitive performances. The loadings of the cognitive indicators demonstrated that swimming distance in the MWM, PI in the NLR, and the PIo and PIod in the ELM contributed most to the first correlation (see Table 7).

Discussion

Chronic DNJ treatment ameliorated the age-related impairments of the behaviors

This study was designed to evaluate the effects of DNJ on age-related behavioral and biochemical changes in the SAMP8 mice. Consistent with previous reports (Markowska et al. 1998b; Takeda 2009), the old P8

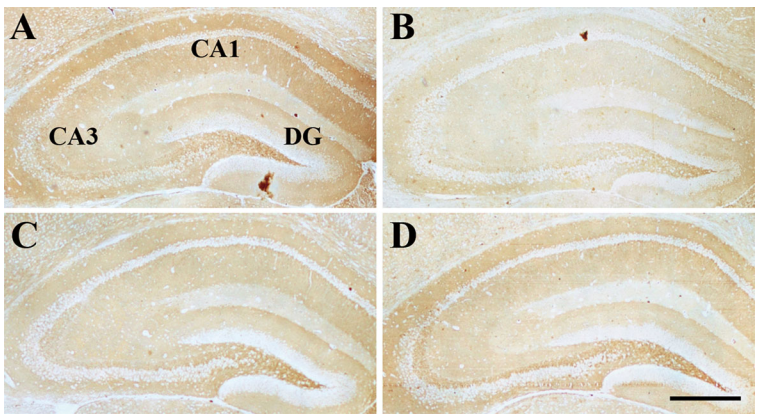

Fig. 6 Effect of age or DNJ on synaptotagmin-1 immunohistochemical staining in the dorsal hippocampus. Representative low-magnification photos in the O-con (**a**), Y-con (**b**), HD-DNJ (**c**), and LD-DNJ (**d**) groups are shown. Synaptotagmin-1 immunoreaction was mainly detected in the DG-HL, CA1-OL, and CA3-OL. The analysis of average optical density showed that the staining for synaptotagmin-1 was more intense in most layers of the old controls than the young controls and the DNJ mice. *DG* dentate gyrus, *HL* hilus, *OL* original layer. *Scale bar*=400 μm

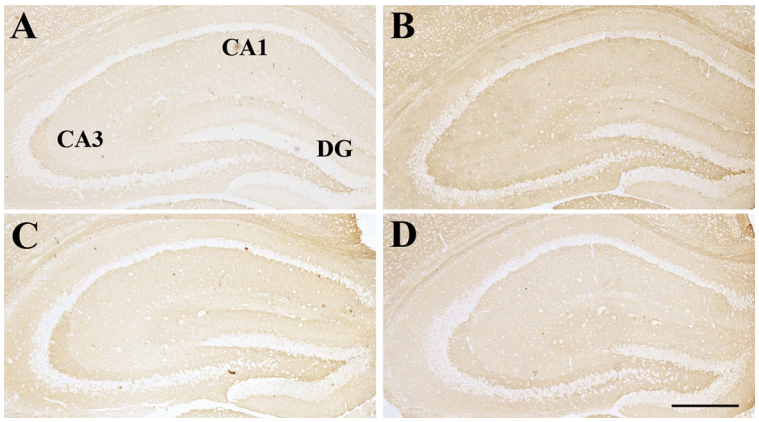

Fig. 7 Effect of age or DNJ on syntaxin-1 immunohistochemical staining in the dorsal hippocampus. Representative low-magnification photos from the O-con (**a**), Y-con (**b**), HD-DNJ (**c**), and LD-DNJ (D) groups are shown. The old mice showed an age-related decrease in syntaxin-1 level in the DG-HL, DG-GL, CA1-RL, CA1-PL, and CA3-ML. The DNJ-treated mice showed a higher syntaxin-1 level in the hippocampal layers compared to the old controls. *DG* dentate gyrus, *GL* granule cell layer, *HL* hilus, *ML* molecular layer, *PL* pyramidal cell layer, *RL* radiation layer. *Scale bar*=400 μm

mice exhibited impairments of sensorimotor skill, decrease of anxiety, and deficits of learning and memory ability. Fortunately, long-term treatment with DNJ could alleviate these age-related behavioral impairments.

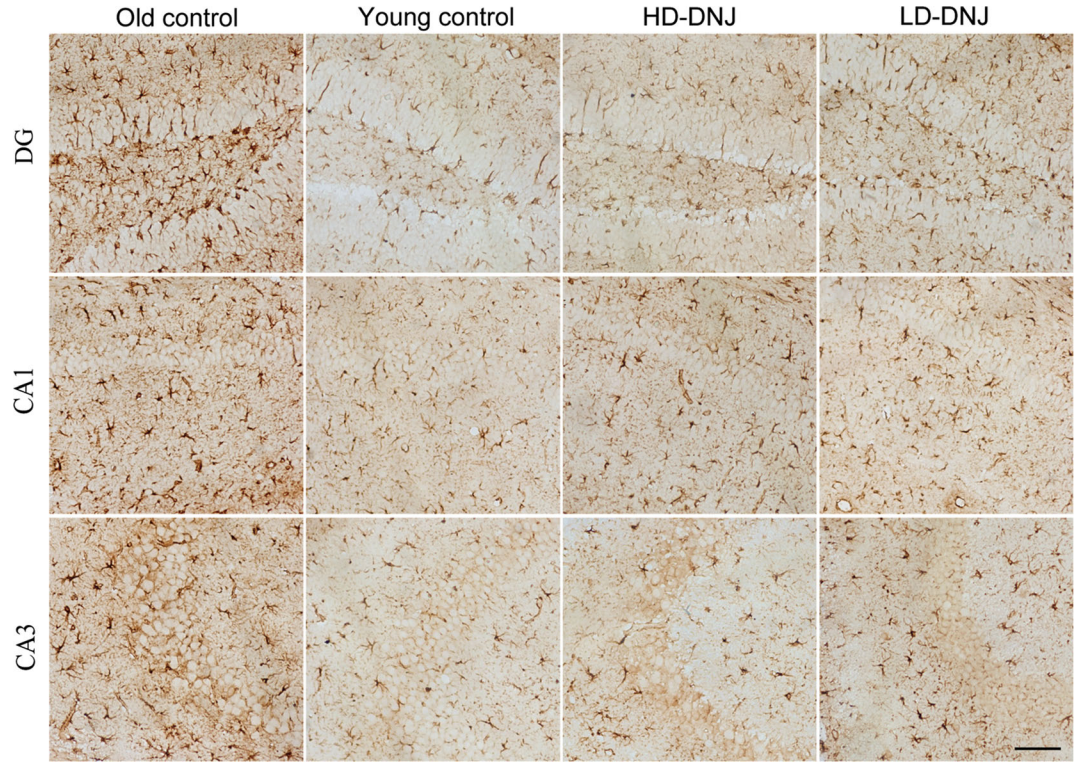

Fig. 8 Effect of age or DNJ on GFAP immunohistochemical staining in the dorsal hippocampus. Representative high-magnification (×20) photos in the hippocampal subregions (DG, CA1, and CA3) in each group are shown. The old SAMP8 mice showed a higher GFAP immunoreactivity in the subregions. The GFAP-positive astrocytes in the old hippocampus were morphologically hypertrophic with enlarged processes, indicating activation of the astrocytes. DNJ treatment significantly relieved the astrocyte activation. *DG* dentate gyrus. *Scale bar*=100 μm

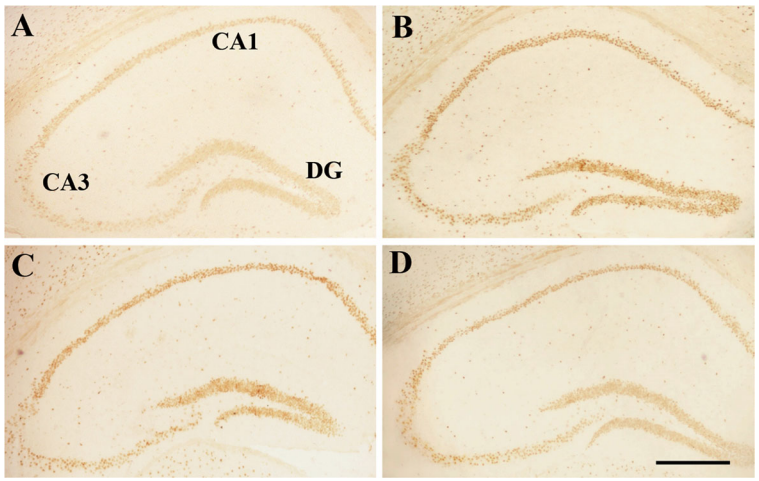

Fig. 9 Effect of age or DNJ on H4K8ac immunohistochemical staining in the dorsal hippocampus. Representative low-magnification images from the O-con (**a**), Y-con (**b**), HD-DNJ (**c**), and LD-DNJ (**d**) groups are shown. The H4K8ac immunoreaction can be observed in the layers that contain the cell bodies of dentate granule cells or pyramidal neurons. The O-con showed a decrease in the H4K8ac level in the DG-GL, CA1-PL, and CA3-PL compared to the Y-con. The decrease was alleviated by the DNJ treatment, especially by the HD-DNJ. *DG* dentate gyrus, *GL* granule cell layer, *PL* pyramidal cell layer. *Scale bar*=400 μm

In this study, to evaluate the sensorimotor ability, we used the tightrope and beam walking tasks. The old P8 mice, especially the males, exhibited impaired sensorimotor performance in both tests. High doses of DNJ alleviated the impairment in both tasks, while low-dose DNJ only exhibited a protective effect in the tightrope task, which may be because the tightrope is more sensitive to sensorimotor deficits (Chen et al. 2004). The reduced swimming velocity of the old P8 mice in the MWM also indicated impaired sensorimotor ability, which was not relieved by DNJ. The anxiety level may also play a role in the reduced swimming velocity, suggested by a study that had reported a decreased motivation to escape from the water in P8 mice (Takeda 2009). Studies of P8 have shown an age-related reduction of anxiety in food neophobia and the water-lick conflict tests (Miyamoto et al. 1992; Takeda 2009). To test the locomotor activity and anxiety level, the open-field task was used in the present study. The O-con showed a lower locomotor activity, as indicated by the fewer number of squares crossed, and a decrease in alertness and anxiety level, as demonstrated by a shorter latency to leave the first square. However, our previous study of SAMP8 found no age effect on open-field anxiety, which could be explained by the fact that only the peripheral time was detected (Chen et al. 2007a). The HD-DNJ treatment, but not the LD-DNJ, could partly relieve the decrease in anxiety.

During aging, many aspects of memory abilities could be impaired, especially spatial learning and memory. In our previous study, P8 mice showed a decreased spatial learning capacity in the MWM at 8 months of age and additional deterioration thereafter (Chen et al. 2007b). The NLR is also a sensitive test for the detection

Table 5 Pearson's correlation coefficient between memory performance and serological results

	Morris water maze		Novel object recognition	Novel location recognition	Episodic-like memory	
	Swimming distance	% of distance in target quadrant	PI	PI	PIo	PIod
Glucose	0.01	0.04	−0.06	−0.10	−0.08	0.07
Insulin	0.22	−0.13	0.19	0.38*	0.41*	0.57**
BDNF	−0.10	0.14	0.36*	0.24	−0.02	0.01
IGF-1	−0.10	−0.15	0.35*	0.23	0.09	−0.06

*$P<0.05$; **$P<0.01$

Table 6 Correlations between InsR in each hippocampal layer and memory ability

Groups	Layers in subregions	Morris water maze		Novel object recognition	Novel location recognition	Episodic-like memory	
		Swimming distance *r* (*P*)	%of distance in the target quadrant *r* (*P*)	PI *r* (*P*)	PI *r* (*P*)	PIo *r* (*P*)	PIod *r* (*P*)
All mice	DG-HL	−0.427** (0.002)	0.469** (0.001)	0.243 (0.085)	0.150 (0.293)	0.252 (0.074)	0.089 (0.534)
	DG-GL	−0.373** (0.007)	0.423** (0.002)	0.357* (0.010)	0.376** (0.007)	0.432** (0.002)	0.346* (0.013)
	DG-ML	−0.480** (0.000)	0.478** (0.000)	0.251 (0.076)	0.336* (0.016)	0.371** (0.007)	0.167 (0.242)
	CA1-ML	−0.627** (0.000)	0.360** (0.009)	0.463** (0.001)	0.227 (0.110)	0.358* (0.010)	0.050 (0.727)
	CA1-RL	−0.563** (0.000)	0.364** (0.009)	0.409** (0.003)	0.188 (0.186)	0.268 (0.058)	0.013 (0.929)
	CA1-PL	−0.375** (0.007)	0.264 (0.061)	0.477** (0.000)	0.313* (0.026)	0.311* (0.026)	0.215 (0.129)
	CA1-OL	−0.596** (0.000)	0.281* (0.046)	0.526** (0.000)	0.256 (0.070)	0.380** (0.006)	0.426** (0.002)
	CA3-ML	−0.521** (0.000)	0.146 (0.306)	0.388** (0.005)	0.214 (0.131)	0.417** (0.002)	0.169 (0.236)
	CA3-SL	−0.193 (0.175)	−0.012 (0.932)	0.289* (0.040)	0.460** (0.001)	0.124 (0.386)	0.468** (0.001)
	CA3-PL	−0.082 (0.572)	0.025 (0.859)	0.113 (0.428)	0.188 (0.187)	0.448** (0.001)	0.139 (0.329)
	CA3-OL	−0.395** (0.005)	0.076 (0.602)	0.307* (0.032)	0.142 (0.329)	0.185 (0.204)	0.107 (0.462)
O-con	DG-HL	−0.277 (0.442)	0.992** (0.000)	−0.453 (0.210)	−0.391 (0.308)	−0.585 (0.078)	−0.084 (0.743)
	DG-ML	−0.195 (0.589)	0.860** (0.003)	−0.207 (0.410)	0.070 (0.848)	−0.358 (0.344)	−0.006 (0.849)
	CA1-ML	−0.725* (0.015)	0.187 (0.558)	0.394 (0.284)	−0.183 (0.594)	−0.142 (0.667)	0.142 (0.676)
Y-con	CA1-PL	0.189 (0.626)	0.704* (0.011)	0.281 (0.401)	−0.450 (0.142)	0.019 (0.958)	0.223 (0.501)
	CA1-OL	−0.643* (0.024)	0.158 (0.624)	0.179 (0.579)	0.173 (0.592)	0.528 (0.078)	0.414 (0.181)
HD-DNJ	DG-GL	0.219 (0.458)	−0.034 (0.907)	0.803** (0.001)	0.229 (0.431)	−0.068 (0.817)	0.123 (0.676)
	CA1-RL	−0.361 (0.205)	−0.067 (0.820)	0.679** (0.008)	0.036 (0.902)	−0.072 (0.806)	0.744** (0.002)
	CA1-OL	−0.629* (0.016)	0.151 (0.605)	0.576 (0.031)	−0.119 (0.685)	−0.325 (0.257)	0.788** (0.001)
LD-DNJ	DG-ML	0.016 (0.961)	−0.360 (0.250)	0.755** (0.005)	0.150 (0.641)	0.442 (0.151)	0.444 (0.149)
	CA1-PL	−0.373 (0.232)	0.526 (0.079)	0.807** (0.002)	−0.353 (0.261)	−0.199 (0.536)	−0.160 (0.620)

PI preference index for novel object in the NOR or for novel location in the NLR, *PIo* preference index for old objects, *PIod* preference index for displaced old object

*$P<0.05$, ** $P<0.01$ denote significant correlation coefficients

Table 7 Canonical loadings and cross loadings for the first correlation between the indicators of insulin/IGF-1 and BDNF system and the performances of memory tests

Items	Tasks	Measures	Canonical loadings	Cross loadings
Serum		Glucose	−0.127	−0.109
		Insulin	0.232	0.198
		BDNF	0.321	0.274
		IGF-1	0.478	0.407
Hippocampus		IGF-1R	−0.555	−0.473
		InsR	0.668	0.570
		BDNF	0.247	0.210
Memory tests	MWM	Swimming distance	−0.667	−0.569
		% of distance in target quadrant	0.138	0.117
	ELM	PIo	0.361	0.307
		PIod	0.257	0.219
	NOR	PI	0.802	0.683
	NLR	PI	0.462	0.394

of hippocampus-dependent spatial learning and memory ability (Murai et al. 2007). Aged CD1 mice display the location memory deficits relative to the young mice (Murai et al. 2007). Poorer performance in the NLR has also been reported in mice on a high-fat diet (Heyward et al. 2012). Although the procedure is similar to NLR, NOR is a nonspatial task in which the identity rather than the location of object is changed (Forwood et al. 2005). In the present study, the old controls exhibited impaired spatial learning and memory in the MWM and the 10-min phase of the NLR test. In the MWM, HD-DNJ ameliorated the age-related decline of spatial learning and memory in both phases, while LD-DNJ only improved the performance in the place learning phase, but not in the probe phase, which is a test for the evaluation of memory retention. Both HD- and LD-DNJ relieved the age-related decline of short-term location memory in the NLR. Similarly, chronic exercise has been reported to improve the NLR performance in aged mice (Snigdha et al. 2014). During the 10-min phase in the NOR task, the O-con showed impairment in distinguishing the new object from the familiar one, which may indicate a degeneration of the perirhinal cortex which is required for NOR. This age-related

Table 8 Canonical loadings and cross loadings for the first correlation between the age-related indicators and the performances of memory tests

		Canonical loadings	Cross loadings
Age-related indicators			
	Syt-1	−0.718	−0.604
	Stx-1	0.732	0.616
	H4K8ac	0.873	0.735
	GFAP	−0.552	−0.465
Cognitive performances			
MWM	Swimming distance	−0.631	0.136
	% of distance in target quadrant	0.108	−0.204
ELM	PIo	0.889	0.169
	PIod	0.670	0.229
NOR	PI	0.216	0.527
NLR	PI	0.595	0.084

deficit in short-term object recognition memory was also relieved by DNJ treatment.

Episodic memory refers to the conscious recollection of a unique past experience in terms of "what" happened and "where" and "when" it happened (DeVito and Eichenbaum 2010). Similar to human, normal rats and mice are capable of encoding episodic-like information. To evaluate the episodic-like memory in mice, we used an apparatus devised by Dere et al. that contains the three elements "what" (object identity), "when" (temporal order of object presentation), and "where" (object displacement) (Dere et al. 2005). The Y-con had a memory of the object seen, where it was located, and when it saw it (in the first or second sample trial). However, the O-con displayed no preference when exploring the objects, indicating an impairment of episodic-like memory, which may be attributed to the age-related degeneration of the hippocampus (DeVito and Eichenbaum 2010) and perirhinal cortex (Barker et al. 2007). The DNJ-treated mice could discriminate previously explored objects and memorize the spatial displacement of objects and had higher PIo and PIod values than the O-con, indicating a protective role of DNJ in the episodic-like memory in the P8 mice.

Chronic DNJ treatment alleviated the age-related changes in the insulin system

During aging, the glucose-induced insulin secretion and sensitivity of insulin reduce in normal elderly and in diabetes patients (Szoke et al. 2008; Oya et al. 2014). Although most studies reported no change or an increase of fasting insulin in aged human and some rodent models (Irwin et al. 2006; Fan et al. 2011; Ribeiro et al. 2012), our nonfasted old SAMP8 mice had relatively lower serum insulin levels. The insulin level could be influenced by different strains, diet, the state of obesity and fitness, and the concentrations of glucagon, growth hormone, and cortisol (Basu et al. 2003). The age-related decrease of the serum insulin level in the P8 mice in this study might be attributed to the decrease in insulin synthesis and secretion in pancreatic islet β cells during aging, as the P8 mouse is a model with accelerated aging processes. In the adult brain, insulin is scarcely produced locally and depends on the transportation of peripheral insulin crossing the blood-brain barrier (Laron 2009; Bosco et al. 2011). Thus, the lower serum insulin level of the O-con might lead to insulin deficiency or declined insulin signaling in the brain (Bosco et al. 2011).

Several studies found that decreased InsR in the brain was associated with cognitive impairment in AD patients and in animal models of diabetes or normal aging (Zhao et al. 1999; Hoyer et al. 2000; Steen et al. 2005; Wang et al. 2010b). Intranasally administered insulin could enhance the membrane expression of InsR on hippocampal neurons and improve learning and memory (Benedict et al. 2007). In our study, the decreased InsR content in the aged hippocampus might indicate an age-related decline in insulin signaling. Furthermore, the decreased InsR content was correlated with the decline in learning and memory (Tables 6 and 7).

Our results showed that DNJ could elevate the serum insulin level and InsR content in most hippocampal layers in the old P8 mice. DNJ is a potent inhibitor of α-glucosidase that reduces the absorption of monosaccharides in the intestine and decreases the blood glucose in human and hyperglycemic or diabetic rodent models (Kimura et al. 2007; Kong et al. 2008; Li et al. 2011). DNJ may also exert a glucose-lowering effect by increasing the action of adiponectin and glucose transporter 4 (Lee et al. 2013). Furthermore, DNJ facilitates insulin sensitivity and reduces body weight in a model of type 2 diabetes, Otsuka Long-Evans Tokushima Fatty rats (Kong et al. 2008). Hybrid treatment of DNJ and polysaccharide from mulberry leaves modulated hepatic glucose metabolism and upregulated insulin expression in the pancreas (Li et al. 2011). In this study, age had no significant effect on the serum concentration of glucose. DNJ did not affect the level of serum glucose perhaps because the old P8 mice did not have hyperglycemia. The mechanism of DNJ affecting the serum insulin level and hippocampal InsR level is unknown. Epigenetic alterations might participate, affecting insulin sensitivity and ameliorating pancreatic stress.

DNJ alleviated the reduction of IGF-1R and BDNF in the aged hippocampus

IGF-1 is a trophic factor with structural and functional homologies to insulin. It activates glucose transport and promotes neurogenesis and angiogenesis in the hippocampus, protecting the brain from vascular dementia and AD (Gong et al. 2012; Torres Aleman 2012). Previous studies have observed that the brain and plasma IGF-1 levels decrease with aging and are associated with age-related impairments of cognitive function,

which can be reversed by exogenous IGF-1 administration (Markowska et al. 1998a; Muller et al. 2012). In our results, although age exerted no effect on the serum IGF-1 level, the DNJ treatment enhanced the serum IGF-1 level in the aged SAMP8 mice. Our old SAMP8 mice exhibited an increased IGF-1R level in the hippocampus, consistent with previous studies on aged rats (Chung et al. 2002; Moloney et al. 2010), and the increased IGF-1R correlated with the cognitive impairment. Increased IGF-1R in the brain may be related to markedly reduced IGF-1/insulin signaling (Muller et al. 2012). Therefore, the increased IGF-1R level might represent a compensatory response to IGF-1/insulin resistance, and DNJ alleviated this increase in IGF-1R probably through relieving IGF-1/insulin resistance. However, studies have linked low IGF-1 signaling to extended longevity, suggesting that IGF-1 signaling plays a complex role in the brain aging process and requires further research (Kappeler et al. 2008).

BDNF is a vital neurotrophin that modulates energy metabolism and the survival and plasticity of neurons (Mattson et al. 2004). Both peripheral and brain-expressed BDNFs in laboratory rodents decrease during normal aging (Rothman et al. 2012). Serum BDNF readily crossed the blood-brain barrier, and the serum level can be affected by the brain BDNF content (Lommatzsch et al. 2005). The hippocampal BDNF level decreases with age, accounting for the age-related decline in learning and memory (Schaaf et al. 2001; Nagahara and Tuszynski 2011). In our results, although no significant effect of aging was displayed, the serum BDNF level was elevated by the DNJ treatment. Our old controls exhibited a decrease in BDNF in the different hippocampal layers, which was correlated with the age-related memory deficits. The DNJ, especially the HD-DNJ, treatment alleviated the age-related decline of BDNF in the hippocampus. Similar findings have been reported in models of physical exercise or caloric restriction, in which the expression of BDNF in the brain is enhanced and associated with ameliorated age-related deficits in hippocampal neuroplasticity (Duan et al. 2001; Intlekofer and Cotman 2013).

DNJ ameliorated the alterations of Syt-1 and Stx-1 levels in the old hippocampus

Syt-1, a major Ca^{2+} sensor in the presynaptic active zone, triggers fast, synchronous fusion of synaptic vesicles by interacting with SNARE (soluble *N*-ethylmaleimide-sensitive factor attachment protein receptor) proteins (Paddock et al. 2011). Stx-1, one of the SNARE proteins, is involved in synaptic vesicle docking and fusion (Quick 2006). Both Syt-1 and Stx-1 play critical roles in the regulation of neurotransmission. An increased Syt level in the hippocampus in the hippocampus of old Wistar rats has been reported (Shimohama et al. 1998). There are also studies in rodents showing contradictory results, where Syt was decreased or unchanged with aging (Nicolle et al. 1999; Jiang et al. 2001). In our previous study, the 8- and 13-month-old P8 mice displayed increased hippocampal Syt-1 expression (Chen et al. 2007b). In this study, we also found elevated levels of Syt-1 in most layers of different hippocampal subregions in the aged P8 mice. Decreased Stx-1 in the brain has been reported in aged normal rodents and transgenic AD mice (Oakley et al. 2006; VanGuilder et al. 2010). Demented human individuals also have lower gene expression levels of Stx in the superior temporal gyrus relative to the nondemented controls, and the Stx levels decreased with age (Beeri et al. 2012). Consistent with these studies, this study found the aged P8 mice had less Stx-1 in different hippocampal layers. Furthermore, the increased Syt-1 and decreased Stx-1 in the hippocampus were associated with the age-related impairment of memory. Chronic DNJ treatment alleviated the changes in Syt-1 and Stx-1 in the hippocampus of old P8 mice. However, the mechanism is unclear and the epigenetic changes during chronic treatment with DNJ may be involved. In addition, the decreased expression of BDNF may affect the content of Stx-1 as well.

DNJ alleviated the increase of GFAP in the old hippocampus

There is a growing body of literature on the role of exaggerated neuroinflammation in normal aging and age-related cognitive decline (Simen et al. 2011). During aging, microglia and astrocytes, the two major cell effectors, contribute to the chronic activation of neuroinflammation and overexpression of proinflammatory cytokines and reactive oxygen species, leading to a decline in long-term potentiation and cognitive dysfunction (Simen et al. 2011; Bilbo et al. 2012). To determine whether DNJ affects age-related astrocyte activation, we analyzed the immunoreactivity of GFAP, an astrocyte-specific intermediate filament component, in the SAMP8 mice. The O-con mice exhibited increased

GFAP in most hippocampal layers and the GFAP-positive astrocytes were morphologically hypertrophic with enlarged processes (Fig. 6), representing astrocyte activation during aging. Increased levels of proinflammatory cytokines secreted by astrocytes, such as TNF-α, IL-1, and IL-6, may interfere with the phosphorylation of the insulin receptor substrate and impair insulin signaling, leading to insulin resistance and neural dysfunction (De Felice and Ferreira 2014). The abnormal insulin system may conversely affect neuroinflammation. For example, in the SAMP8 mice with streptozotocin-induced type 1 diabetes, the decline in insulin in the hippocampus leads to astrogliosis (Currais et al. 2012). Increased GFAP has also been reported in aged rats and patients and animal models of AD (Heneka et al. 2005; Zhang et al. 2012). In the present study, elevated GFAP level was closely related with the declined memory ability. The chronic DNJ treatment attenuated the age-related astroglial activation in the hippocampus, as indicated by the decreased GFAP level. The protective effect of DNJ on the memory abilities might be associated with the suppressed inflammation in the hippocampus.

DNJ alleviated alterations in H4K8ac in the old hippocampus

Histone acetylation induces the transcription and synthesis of proteins required for the formation of long-term memory by directly recruiting other proteins or destabilizing the interaction between histones and DNA (Peleg et al. 2010). Deacetylation by HDAC inhibits memory ability. The activity of HAT and HDAC controls the level of histone acetylation and thus affects cognitive ability. Several HDAC inhibitors have been shown to be potential enhancers of cognition in patients with neurodegenerative disease and cognitively healthy adults (Graff and Tsai 2013). HDAC inhibitors, sodium butyrate (NaB), pentyl-4-yn-VPA, and suberoylanilide hydroxamic acid (SAHA) can enhance the acetylation status of H4K8 in the hippocampus, which improves the gene expression necessary for synaptic plasticity and memory formation (Itzhak et al. 2013; Foley et al. 2014). Intlekofer et al. reported that NaB treatment leads to an increase in BDNF transcripts I and IV, associated with BDNF promoter acetylation on H4K8 (Intlekofer et al. 2013). Our O-con mice showed decreased levels of H4K8ac in the cell layers of the hippocampus, which was alleviated by the DNJ treatment (Table 4). HD-DNJ was more effective in elevating the H4K8ac relative to LD-DNJ. Higher H4K8ac level correlated with better performance in the memory tests (Table 8). H4K8 acetylation might be an important epigenetic mechanism by which DNJ enhances hippocampal-dependent learning and memory. However, in this study, we did not investigate whether the level of histone acetylation directly affects the gene transcription and translation of insulin, IGF-1R, BDNF, and synaptic proteins. Further study is needed to clarify the effect of histone acetylation on the expression of specific brain aging-related genes.

The canonical correlation analysis revealed that the age-related changes in serological tests and protein content in the hippocampal layers were closely related to the impairment of learning and memory abilities. Among the indicators of learning and memory, the impairments of the learning (swimming distance) in the MWM and the memory (PI) in the NOR were most attributable to the changes of the insulin/IGF-1 and BDNF system. However, the impairments of the learning (swimming distance) in the MWM and the memory (PIs) in the NLR and ELM were most attributable to the age-related changes of Syt-1, Stx-1, GFAP, and H4K8ac. Interestingly, the impairment of memory (target-quadrant distance %) in the MWM was not attributable to the alterations of the hippocampal proteins in this study. These results might be helpful for the choice of parameters when researching the relationships between cognitive changes and hippocampal proteins mentioned in this study.

In summary, the present study is the first to explore the relieving effect of DNJ on the age-related behavioral changes by a series of behavioral tests of motor ability, anxiety, spatial and nonspatial learning, and memory abilities. The DNJ treatment (especially at the higher dose) could alter several age-related markers in older SAMP8 mice to yield characteristics similar to those seen in young mice. Among these behavior tests, the age-related deficits in the Morris water maze and the episodic-like memory test were significantly reversed by DNJ administration. In the NOR and NLR, only the short-term memory was affected. Among the biochemical indicators, InsR, Syt-l, GFAP, and H4K8ac more consistently showed a trend toward values seen in young SAMP8 after DNJ treatment. The relative levels of IGF-R, BDNF, and Stx-l showed a significant change following DNJ treatment only in some regions. To sum up, InsR and H4K8ac may be the most representative and preferred indicators in a future study.

Compared to the acarbose in our previous study (Tong et al. 2015), the DNJ showed a similar protective effect on the brain aging. However, long-term treatment with DNJ elevated the serum IGF-1 and BDNF levels in the aged P8 mice, while the acarbose treatment did not have this effect. The difference may be due to that the mechanisms of acarbose and DNJ are not identical. In addition, DNJ has more application advantages than acarbose. DNJ is widely distributed in a variety of plants and microorganisms and can be easily obtained through an extraction process. Therefore, DNJ is more natural and safe, can be used as a food additive in routine health care, and has a broader prospect for the application in alleviating age-related behavioral changes. The study proposed the potential of DNJ in the treatment of brain aging and showed a preliminary exploration of this potential. Further research using advanced methods is required for more specific mechanisms of the function of DNJ in the aging brain.

Acknowledgments This work was financially supported by the National Foundation of Nature Science of China (81370444), the Natural Science Foundation for the Youth of China (81301094), the Special Fund for Agro-scientific Research in the Public Interest of China (No. 201403064), and the key project of the Natural Science from the Education Department of Anhui Province (ZD2008007-1 and 2).

Conflict of interest The authors declare that they have no competing interests.

References

Abbott MA, Wells DG, Fallon JR (1999) The insulin receptor tyrosine kinase substrate p58/53 and the insulin receptor are components of CNS synapses. J Neurosci 19:7300–7308

Ahlskog JE, Geda YE, Graff-Radford NR, Petersen RC (2011) Physical exercise as a preventive or disease-modifying treatment of dementia and brain aging. Mayo Clin Proc 86:876–884

Anton SD, Karabetian C, Heekin K, Leeuwenburgh C (2013) Caloric restriction to moderate senescence: mechanisms and clinical utility. Curr Transl Geriatr Exp Gerontol Rep 2:239–246

Avogaro A, de Kreutzenberg SV, Fadini GP (2010) Insulin signaling and life span. Pflugers Arch 459:301–314

Balzarini J (2007) The alpha(1,2)-mannosidase I inhibitor 1-deoxymannojirimycin potentiates the antiviral activity of carbohydrate-binding agents against wild-type and mutant HIV-1 strains containing glycan deletions in gp120. FEBS Lett 581:2060–2064

Barker GR, Bird F, Alexander V, Warburton EC (2007) Recognition memory for objects, place, and temporal order: a disconnection analysis of the role of the medial prefrontal cortex and perirhinal cortex. J Neurosci 27:2948–2957

Barzilai N, Huffman DM, Muzumdar RH, Bartke A (2012) The critical role of metabolic pathways in aging. Diabetes 61: 1315–1322

Basu R, Breda E, Oberg AL, Powell CC, Dalla MC, Basu A, Vittone JL, Klee GG, Arora P, Jensen MD, Toffolo G, Cobelli C, Rizza RA (2003) Mechanisms of the age-associated deterioration in glucose tolerance: contribution of alterations in insulin secretion, action, and clearance. Diabetes 52:1738–1748

Beeri MS, Haroutunian V, Schmeidler J, Sano M, Fam P, Kavanaugh A, Barr AM, Honer WG, Katsel P (2012) Synaptic protein deficits are associated with dementia irrespective of extreme old age. Neurobiol Aging 33(1125): e1121–1128

Benedict C, Hallschmid M, Schultes B, Born J, Kern W (2007) Intranasal insulin to improve memory function in humans. Neuroendocrinology 86:136–142

Bilbo SD, Smith SH, Schwarz JM (2012) A lifespan approach to neuroinflammatory and cognitive disorders: a critical role for glia. J Neuroimmune Pharmacol 7:24–41

Bosco D, Fava A, Plastino M, Montalcini T, Pujia A (2011) Possible implications of insulin resistance and glucose metabolism in Alzheimer's disease pathogenesis. J Cell Mol Med 15:1807–1821

Chen GH, Wang C, Yangcheng HY, Liu RY, Zhou JN (2007a) Age-related changes in anxiety are task-specific in the senescence-accelerated prone mouse 8. Physiol Behav 91: 644–651

Chen GH, Wang H, Yang QG, Tao F, Wang C, Xu DX (2011) Acceleration of age-related learning and memory decline in middle-aged CD-1 mice due to maternal exposure to lipopolysaccharide during late pregnancy. Behav Brain Res 218: 267–279

Chen GH, Wang YJ, Qin S, Yang QG, Zhou JN, Liu RY (2007b) Age-related spatial cognitive impairment is correlated with increase of synaptotagmin 1 in dorsal hippocampus in SAMP8 mice. Neurobiol Aging 28:611–618

Chen GH, Wang YJ, Zhang LQ, Zhou JN (2004) Age- and sex-related disturbance in a battery of sensorimotor and cognitive tasks in Kunming mice. Physiol Behav 83:531–541

Chung YH, Shin CM, Joo KM, Kim MJ, Cha CI (2002) Region-specific alterations in insulin-like growth factor receptor type I in the cerebral cortex and hippocampus of aged rats. Brain Res 946:307–313

Coelho FG, Gobbi S, Andreatto CA, Corazza DI, Pedroso RV, Santos-Galduroz RF (2013) Physical exercise modulates peripheral levels of brain-derived neurotrophic factor (BDNF): a systematic review of experimental studies in the elderly. Arch Gerontol Geriatr 56:10–15

Currais A, Prior M, Lo D, Jolivalt C, Schubert D, Maher P (2012) Diabetes exacerbates amyloid and neurovascular pathology in aging-accelerated mice. Aging Cell 11:1017–1026

De Felice FG, Ferreira ST (2014) Inflammation, defective insulin signaling, and mitochondrial dysfunction as common molecular denominators connecting type 2 diabetes to Alzheimer disease. Diabetes 63:2262–2272

Dere E, Huston JP, De Souza Silva MA (2005) Episodic-like memory in mice: simultaneous assessment of object, place and temporal order memory. Brain Res Brain Res Protoc 16: 10–19

DeVito LM, Eichenbaum H (2010) Distinct contributions of the hippocampus and medial prefrontal cortex to the "what-where-when" components of episodic-like memory in mice. Behav Brain Res 215:318–325

Driscoll I, Hamilton DA, Petropoulos H, Yeo RA, Brooks WM, Baumgartner RN, Sutherland RJ (2003) The aging hippocampus: cognitive, biochemical and structural findings. Cereb Cortex 13:1344–1351

Duan W, Lee J, Guo Z, Mattson MP (2001) Dietary restriction stimulates BDNF production in the brain and thereby protects neurons against excitotoxic injury. J Mol Neurosci 16:1–12

Fan R, Kang Z, He L, Chan J, Xu G (2011) Exendin-4 improves blood glucose control in both young and aging normal non-diabetic mice, possible contribution of beta cell independent effects. PLoS One 6:e20443

Foley AG, Cassidy AW, Regan CM (2014) Pentyl-4-yn-VPA, a histone deacetylase inhibitor, ameliorates deficits in social behavior and cognition in a rodent model of autism spectrum disorders. Eur J Pharmacol 727:80–86

Forwood SE, Winters BD, Bussey TJ (2005) Hippocampal lesions that abolish spatial maze performance spare object recognition memory at delays of up to 48 hours. Hippocampus 15: 347–355

Gong X, Ma M, Fan X, Li M, Liu Q, Liu X, Xu G (2012) Down-regulation of IGF-1/IGF-1R in hippocampus of rats with vascular dementia. Neurosci Lett 513:20–24

Graff J, Tsai LH (2013) The potential of HDAC inhibitors as cognitive enhancers. Annu Rev Pharmacol Toxicol 53:311–330

Heneka MT, Sastre M, Dumitrescu-Ozimek L, Hanke A, Dewachter I, Kuiperi C, O'Banion K, Klockgether T, Van Leuven F, Landreth GE (2005) Acute treatment with the PPARgamma agonist pioglitazone and ibuprofen reduces glial inflammation and Abeta1-42 levels in APPV717I transgenic mice. Brain 128:1442–1453

Heyward FD, Walton RG, Carle MS, Coleman MA, Garvey WT, Sweatt JD (2012) Adult mice maintained on a high-fat diet exhibit object location memory deficits and reduced hippocampal SIRT1 gene expression. Neurobiol Learn Mem 98: 25–32

Howe JD, Smith N, Lee MJ, Ardes-Guisot N, Vauzeilles B, Desire J, Baron A, Bleriot Y, Sollogoub M, Alonzi DS, Butters TD (2013) Novel imino sugar alpha-glucosidase inhibitors as antiviral compounds. Bioorg Med Chem 21:4831–4838

Hoyer S, Lee SK, Loffler T, Schliebs R (2000) Inhibition of the neuronal insulin receptor. An in vivo model for sporadic Alzheimer disease? Ann N Y Acad Sci 920:256–258

Intlekofer KA, Berchtold NC, Malvaez M, Carlos AJ, McQuown SC, Cunningham MJ, Wood MA, Cotman CW (2013) Exercise and sodium butyrate transform a subthreshold learning event into long-term memory via a brain-derived neurotrophic factor-dependent mechanism. Neuropsychopharmacology 38: 2027–2034

Intlekofer KA, Cotman CW (2013) Exercise counteracts declining hippocampal function in aging and Alzheimer's disease. Neurobiol Dis 57:47–55

Irie F, Fitzpatrick AL, Lopez OL, Kuller LH, Peila R, Newman AB, Launer LJ (2008) Enhanced risk for Alzheimer disease in persons with type 2 diabetes and APOE epsilon4: the Cardiovascular Health Study Cognition Study. Arch Neurol 65:89–93

Irwin N, Green BD, Gault VA, Harriot P, O'Harte FP, Flatt PR (2006) Stable agonist of glucose-dependent insulinotropic polypeptide (GIP) restores pancreatic beta cell glucose responsiveness but not glucose intolerance in aging mice. Exp Gerontol 41:151–156

Islam B, Khan SN, Haque I, Alam M, Mushfiq M, Khan AU (2008) Novel anti-adherence activity of mulberry leaves: inhibition of Streptococcus mutans biofilm by 1-deoxynojirimycin isolated from Morus alba. J Antimicrob Chemother 62:751–757

Itzhak Y, Liddie S, Anderson KL (2013) Sodium butyrate-induced histone acetylation strengthens the expression of cocaine-associated contextual memory. Neurobiol Learn Mem 102: 34–42

Jagust W, Gitcho A, Sun F, Kuczynski B, Mungas D, Haan M (2006) Brain imaging evidence of preclinical Alzheimer's disease in normal aging. Ann Neurol 59:673–681

Jang JS, Cho Y, Jeong GT, Kim SK (2012) Optimization of saccharification and ethanol production by simultaneous saccharification and fermentation (SSF) from seaweed, Saccharina japonica. Bioprocess Biosyst Eng 35:11–18

Jiang CH, Tsien JZ, Schultz PG, Hu Y (2001) The effects of aging on gene expression in the hypothalamus and cortex of mice. Proc Natl Acad Sci U S A 98:1930–1934

Kappeler L, De Magalhaes Filho C, Dupont J, Leneuve P, Cervera P, Perin L, Loudes C, Blaise A, Klein R, Epelbaum J, Le Bouc Y, Holzenberger M (2008) Brain IGF-1 receptors control mammalian growth and lifespan through a neuroendocrine mechanism. PLoS Biol 6:e254

Kimura T, Nakagawa K, Kubota H, Kojima Y, Goto Y, Yamagishi K, Oita S, Oikawa S, Miyazawa T (2007) Food-grade mulberry powder enriched with 1-deoxynojirimycin suppresses the elevation of postprandial blood glucose in humans. J Agric Food Chem 55:5869–5874

Kojima Y, Kimura T, Nakagawa K, Asai A, Hasumi K, Oikawa S, Miyazawa T (2010) Effects of mulberry leaf extract rich in 1-deoxynojirimycin on blood lipid profiles in humans. J Clin Biochem Nutr 47:155–161

Komatsu T, Chiba T, Yamaza H, Yamashita K, Shimada A, Hoshiyama Y, Henmi T, Ohtani H, Higami Y, de Cabo R, Ingram DK, Shimokawa I (2008) Manipulation of caloric content but not diet composition, attenuates the deficit in learning and memory of senescence-accelerated mouse strain P8. Exp Gerontol 43:339–346

Kong WH, Oh SH, Ahn YR, Kim KW, Kim JH, Seo SW (2008) Antiobesity effects and improvement of insulin sensitivity by 1-deoxynojirimycin in animal models. J Agric Food Chem 56:2613–2619

Korol DL, Gold PE (1998) Glucose, memory, and aging. Am J Clin Nutr 67:764S–771S

Lachner M, O'Sullivan RJ, Jenuwein T (2003) An epigenetic road map for histone lysine methylation. J Cell Sci 116:2117–2124

Laron Z (2009) Insulin and the brain. Arch Physiol Biochem 115: 112–116

Lee SM, Do HJ, Shin MJ, Seong SI, Hwang KY, Lee JY, Kwon O, Jin T, Chung JH (2013) 1-Deoxynojirimycin isolated from a Bacillus subtilis stimulates adiponectin and GLUT4 expressions in 3T3-L1 adipocytes. J Microbiol Biotechnol 23:637–643

Li YG, Ji DF, Zhong S, Lv ZQ, Lin TB, Chen S, Hu GY (2011) Hybrid of 1-deoxynojirimycin and polysaccharide from mulberry leaves treat diabetes mellitus by activating PDX-1/insulin-1 signaling pathway and regulating the expression of glucokinase, phosphoenolpyruvate carboxykinase and glucose-6-phosphatase in alloxan-induced diabetic mice. J Ethnopharmacol 134:961–970

Lommatzsch M, Zingler D, Schuhbaeck K, Schloetcke K, Zingler C, Schuff-Werner P, Virchow JC (2005) The impact of age, weight and gender on BDNF levels in human platelets and plasma. Neurobiol Aging 26:115–123

Luger K, Mader AW, Richmond RK, Sargent DF, Richmond TJ (1997) Crystal structure of the nucleosome core particle at 2.8 A resolution. Nature 389:251–260

Markowska AL, Mooney M, Sonntag WE (1998a) Insulin-like growth factor-1 ameliorates age-related behavioral deficits. Neuroscience 87:559–569

Markowska AL, Spangler EL, Ingram DK (1998b) Behavioral assessment of the senescence-accelerated mouse (SAM P8 and R1). Physiol Behav 64:15–26

Mattson MP, Maudsley S, Martin B (2004) A neural signaling triumvirate that influences ageing and age-related disease: insulin/IGF-1, BDNF and serotonin. Ageing Res Rev 3:445–464

Miyamoto M, Kiyota Y, Nishiyama M, Nagaoka A (1992) Senescence-accelerated mouse (SAM): age-related reduced anxiety-like behavior in the SAM-P/8 strain. Physiol Behav 51:979–985

Moloney AM, Griffin RJ, Timmons S, O'Connor R, Ravid R, O'Neill C (2010) Defects in IGF-1 receptor, insulin receptor and IRS-1/2 in Alzheimer's disease indicate possible resistance to IGF-1 and insulin signalling. Neurobiol Aging 31:224–243

Muller AP, Fernandez AM, Haas C, Zimmer E, Portela LV, Torres-Aleman I (2012) Reduced brain insulin-like growth factor I function during aging. Mol Cell Neurosci 49:9–12

Murai T, Okuda S, Tanaka T, Ohta H (2007) Characteristics of object location memory in mice: behavioral and pharmacological studies. Physiol Behav 90:116–124

Nagahara AH, Tuszynski MH (2011) Potential therapeutic uses of BDNF in neurological and psychiatric disorders. Nat Rev Drug Discov 10:209–219

Nagashima K, Zabriskie JB, Lyons MJ (1992) Virus-induced obesity in mice: association with a hypothalamic lesion. J Neuropathol Exp Neurol 51:101–109

Nakagawa K, Kubota H, Tsuzuki T, Kariya J, Kimura T, Oikawa S, Miyazawa T (2008) Validation of an ion trap tandem mass spectrometric analysis of mulberry 1-deoxynojirimycin in human plasma: application to pharmacokinetic studies. Biosci Biotechnol Biochem 72:2210–2213

Nicolle MM, Gallagher M, McKinney M (1999) No loss of synaptic proteins in the hippocampus of aged, behaviorally impaired rats. Neurobiol Aging 20:343–348

Oakley H, Cole SL, Logan S, Maus E, Shao P, Craft J, Guillozet-Bongaarts A, Ohno M, Disterhoft J, Van Eldik L, Berry R, Vassar R (2006) Intraneuronal beta-amyloid aggregates, neurodegeneration, and neuron loss in transgenic mice with five familial Alzheimer's disease mutations: potential factors in amyloid plaque formation. J Neurosci 26:10129–10140

Oya J, Nakagami T, Yamamoto Y, Fukushima S, Takeda M, Endo Y, Uchigata Y (2014) Effects of age on insulin resistance and secretion in subjects without diabetes. Intern Med 53:941–947

Paddock BE, Wang Z, Biela LM, Chen K, Getzy MD, Striegel A, Richmond JE, Chapman ER, Featherstone DE, Reist NE (2011) Membrane penetration by synaptotagmin is required for coupling calcium binding to vesicle fusion in vivo. J Neurosci 31:2248–2257

Peleg S, Sananbenesi F, Zovoilis A, Burkhardt S, Bahari-Javan S, Agis-Balboa RC, Cota P, Wittnam JL, Gogol-Doering A, Opitz L, Salinas-Riester G, Dettenhofer M, Kang H, Farinelli L, Chen W, Fischer A (2010) Altered histone acetylation is associated with age-dependent memory impairment in mice. Science 328:753–756

Quick MW (2006) The role of SNARE proteins in trafficking and function of neurotransmitter transporters. Handb Exp Pharmacol, 181-196

Ribeiro RA, Batista TM, Coelho FM, Boschero AC, Lopes GS, Carneiro EM (2012) Decreased beta-cell insulin secretory function in aged rats due to impaired Ca(2+) handling. Exp Physiol 97:1065–1073

Rothman SM, Griffioen KJ, Wan R, Mattson MP (2012) Brain-derived neurotrophic factor as a regulator of systemic and brain energy metabolism and cardiovascular health. Ann N Y Acad Sci 1264:49–63

Schaaf MJ, Workel JO, Lesscher HM, Vreugdenhil E, Oitzl MS, de Kloet ER (2001) Correlation between hippocampal BDNF mRNA expression and memory performance in senescent rats. Brain Res 915:227–233

Shimohama S, Fujimoto S, Sumida Y, Akagawa K, Shirao T, Matsuoka Y, Taniguchi T (1998) Differential expression of rat brain synaptic proteins in development and aging. Biochem Biophys Res Commun 251:394–398

Silverman DH, Small GW, Chang CY, Lu CS, Kung De Aburto MA, Chen W, Czernin J, Rapoport SI, Pietrini P, Alexander GE, Schapiro MB, Jagust WJ, Hoffman JM, Welsh-Bohmer KA, Alavi A, Clark CM, Salmon E, de Leon MJ, Mielke R, Cummings JL, Kowell AP, Gambhir SS, Hoh CK, Phelps ME (2001) Positron emission tomography in evaluation of dementia: regional brain metabolism and long-term outcome. JAMA 286:2120–2127

Simen AA, Bordner KA, Martin MP, Moy LA, Barry LC (2011) Cognitive dysfunction with aging and the role of inflammation. Ther Adv Chronic Dis 2:175–195

Snigdha S, de Rivera C, Milgram NW, Cotman CW (2014) Exercise enhances memory consolidation in the aging brain. Front Aging Neurosci 6:3

Steen E, Terry BM, Rivera EJ, Cannon JL, Neely TR, Tavares R, Xu XJ, Wands JR, de la Monte SM (2005) Impaired insulin and insulin-like growth factor expression and signaling mechanisms in Alzheimer's disease—is this type 3 diabetes? J Alzheimers Dis 7:63–80

Szoke E, Shrayyef MZ, Messing S, Woerle HJ, van Haeften TW, Meyer C, Mitrakou A, Pimenta W, Gerich JE (2008) Effect of aging on glucose homeostasis: accelerated deterioration of beta-cell function in individuals with impaired glucose tolerance. Diabetes Care 31:539–543

Takeda T (2009) Senescence-accelerated mouse (SAM) with special references to neurodegeneration models, SAMP8 and SAMP10 mice. Neurochem Res 34:639–659

Tong JJ, Chen GH, Wang F, Li XW, Cao L, Sui X, Tao F, Yan WW, Wei ZJ (2015) Chronic acarbose treatment alleviates age-related behavioral and biochemical changes in SAMP8 mice. Behav Brain Res 284:138–152

Torres Aleman I (2012) Insulin-like growth factor-1 and central neurodegenerative diseases. Endocrinol Metab Clin N Am 41(395–408):vii

Tsuduki T, Kikuchi I, Kimura T, Nakagawa K, Miyazawa T (2013) Intake of mulberry 1-deoxynojirimycin prevents diet-induced obesity through increases in adiponectin in mice. Food Chem 139:16–23

Tsuruoka T, Fukuyasu H, Ishii M, Usui T, Shibahara S, Inouye S (1996) Inhibition of mouse tumor metastasis with nojirimycin-related compounds. J Antibiot (Tokyo) 49:155–161

Van de Laar FA, Lucassen PL, Akkermans RP, Van de Lisdonk EH, Rutten GE, Van Weel C (2005) Alpha-glucosidase inhibitors for type 2 diabetes mellitus. Cochrane Database Syst Rev CD003639

VanGuilder HD, Farley JA, Yan H, Van Kirk CA, Mitschelen M, Sonntag WE, Freeman WM (2011) Hippocampal dysregulation of synaptic plasticity-associated proteins with age-related cognitive decline. Neurobiol Dis 43:201–212

VanGuilder HD, Yan H, Farley JA, Sonntag WE, Freeman WM (2010) Aging alters the expression of neurotransmission-regulating proteins in the hippocampal synaptoproteome. J Neurochem 113:1577–1588

Wang RJ, Yang CH, Hu ML (2010a) 1-Deoxynojirimycin inhibits metastasis of B16F10 melanoma cells by attenuating the activity and expression of matrix metalloproteinases-2 and -9 and altering cell surface glycosylation. J Agric Food Chem 58:8988–8993

Wang X, Zheng W, Xie JW, Wang T, Wang SL, Teng WP, Wang ZY (2010b) Insulin deficiency exacerbates cerebral amyloidosis and behavioral deficits in an Alzheimer transgenic mouse model. Mol Neurodegener 5:46

Watson GS, Craft S (2003) The role of insulin resistance in the pathogenesis of Alzheimer's disease: implications for treatment. CNS Drugs 17:27–45

Wirths O, Bayer TA (2010) Neuron loss in transgenic mouse models of Alzheimer's disease. Int J Alzheimers Dis 2010

Xavier LL, Viola GG, Ferraz AC, Da Cunha C, Deonizio JM, Netto CA, Achaval M (2005) A simple and fast densitometric method for the analysis of tyrosine hydroxylase immunoreactivity in the substantia nigra pars compacta and in the ventral tegmental area. Brain Res Brain Res Protoc 16:58–64

Zhang R, Kadar T, Sirimanne E, MacGibbon A, Guan J (2012) Age-related memory decline is associated with vascular and microglial degeneration in aged rats. Behav Brain Res 235:210–217

Zhao W, Chen H, Xu H, Moore E, Meiri N, Quon MJ, Alkon DL (1999) Brain insulin receptors and spatial memory. Correlated changes in gene expression, tyrosine phosphorylation, and signaling molecules in the hippocampus of water maze trained rats. J Biol Chem 274:34893–34902

Zhao WQ, Chen H, Quon MJ, Alkon DL (2004) Insulin and the insulin receptor in experimental models of learning and memory. Eur J Pharmacol 490:71–81